Sorbonne Université

Master 2 Sciences de l'Univers, Environnement, Ecologie

Mention Sciences de la Terre, des Planètes et de l'Environnement

Parcours Hydrologie, Hydrogéologie et Géochimie Environnementale

Climate change impact and uncertainty analysis on streamflow projections.

Thibault Lemaitre-Basset

Research Directors: Lila Collet, Guillaume Thirel and Juraj Parajka

1 Febuary 1st 2019 — 30 July 2019

Contents

Abstract

This study investigates climate change impact on hydrological extremes and performs an uncertainty analysis. This work is applied on a French Mediterranean catchment: the Hérault River catchment. With climate change, local water managers need an evaluation of possible future changes in hydro-climatic variables to develop adaptation strategies. This analysis used for the first time climatic projections derived from a new downscaling method: ADAMONT, with two different Radiative Concentration Pathways (RCPs). Hydrological projections are computed with three hydrological models (GR5J, GRSD, TUW) and different parameter sets obtained with 29 calibration strategies. The uncertainty analysis is based on the quasi-ergodic analysis of variance (QE-ANOVA), to evaluate the contribution of general circulation models (GCMs), regional circulation models (RCMs), hydrological models (HMs), hydrological parameters, and the internal variability to the total uncertainty. Results for high-flow projections with RCP 4.5 show a significant increase between 1976-2005 and 2006-2100 (from +5% to +70%), whereas with RCP 8.5 there is no clear trend (from -10% to +60%). These results are significant and robust for RCP 4.5 but not for RCP 8.5, according to the principle of time of emergence. However, for low-flow projections, results are not significant, and no clear trend can be drawn. These results are discussed compared to previous hydrological projections on the same catchment, and reveal a higher increase of high-flows over time. Moreover, the hydrological model and calibration strategy contributions to the total uncertainty could be reduced for future investigations. Conclusions of this study could be used for decision makers of the Hérault River catchment to establish adaptation strategies on flood risk.

1 Introduction

Climate change (CC) impact on water resources is one of the main challenging issues for water managers. The Intergovernmental Panel on Climate Change (IPCC) drew the last conclusions regarding impacts of CC to policy makers in the 4th report (IPCC, 2014). According to the IPCC : "Freshwater-related risks of climate change increase significantly with increasing greenhouse gas concentrations". This conclusion urges stakeholders and decision makers to think water management in a new way. The IPCC identifies key risks about water ressources in Europe: the increase in water restrictions due to a strong reduction in water availability, combined with an increasing water demand. The increase in the evaporative demand causes a decrease in runoff, and this risk is particularly high in southern Europe. Furthermore, the Mediterranean region is described as a CC hot-spot (Diffenbaugh and Giorgi, 2012), where hydro-climatic hazards will increase with CC (Edenhofer et al., 2011). For example the intensity of heavy precipitation events will increase under a warmer climate on the Mediterranean region (Scoccimarro et al., 2016). In this context, the IPCC recommends to adopt more flexible strategies, and creates plannings according to different scenarios, in order to create resilience to uncertain hydrological changes.

The Mediterranean region is facing difficulties in water management: growing population, agricultural irrigation, and intense touristic activities, put high pressure on water resources (Milano et al., 2012). Moreover, in autumn flash-flood events can be devastating. In order to adapt water management plans, decision makers need hydrological projections. Scientists produce hydrological projections for CC impact studies through a modeling chain, and show how CC can strongly modify spatial and temporal distribution of water resources (Schewe et al., 2014; Haddeland et al., 2014) and hydro-hazards (Collet et al., 2017).

These regional difficulties are particularly tangible on the Hérault River catchment according to the water management plan (http://www.fleuve-herault.fr/). According to the regional water management report (www.eaurmc.fr, 2014), the Héraut River catchment shows a high vulnerability to climatic and antropogenic change. Moreover in a changing climate context, Collet et al. (2015) evaluated water sustainability on the Hérault River catchment with an integrative modeling approach. Conclusions are clear: under a non-mitigation scenario, water resources sustainability will be strongly impacted, and reflections on strict water restriction management are now being developed. However, the hydrological projections have the same order of magnitude as the uncertainty, which causes difficulties in the interpretation of results and on the best adaptation strategies to adopt. Estimating uncertainties at each step of the impact modeling chain and the natural variability of the climate system is an essential task, broached mainly in the literature over recent years (see e.g. Hattermann et al., 2018).

This study aims to assess hydrological changes and to quantify each uncertainty sources across the impact modeling chain, with the use of innovative and effective methods. In this study, we will address the following research questions: 1) What is the impact of CC on hydrological extremes in the Hérault River catchment using recent climatic projections? 2) What is the magnitude of uncertainties and where do they come from ? 3) Can we draw conclusions for the decision makers ?

2 Bibliography

2.1 Climate change impact studies in hydrology

2.1.1 Results of previous impact studies

Explore 2070 (Chauveau et al., 2013) is a reference project on CC impact on river flow over France. Results of this study are key to inform decision-makers and develop adaptation strategies. This report pays particular attention to the quantification of uncertainties. The assumption of a stationary state of the catchment physical properties catchment is one of the main problems: it supposes that the bias of the hydrological model today is the same in the future. However, this study did not investigate all possible uncertainty sources, such as the gas emission scenario and the downscaling process. This report shows two main trends over France: a decrease in precipitation (16% to 23%), and a decrease in streamflow particularly for low-flows. Similarly, the R2D2 2050 project (Sauquet, 2015), is a CC impact study focusing on the Durance River catchment, in the southeast of France. The authors noticed a strong uncertainty about change in precipitations, correlated to a strong uncertainty on streamflow in winter. A major decrease in streamflow to the future is expected in summer or, in other words, a decrease in water resources. Both projects highlighted the challenges induced by uncertainty quantification in a multi-model approach. Previous climate impact studies on Mediterranean catchments indicate an impact on the hydrological regime related to the physical characteristics of the catchment (Sellami et al., 2016), more frequent and longer low flows according to a decrease in precipitation (Piras et al., 2014), and a significant decrease in streamflow, wich depends on the calibration procedure of the hydrological modeling (Lespinas et al., 2014). According to these studies, the current methodology for uncertainty quantification in impact studies is based on a modeling chain in three steps: CC projection, downscaling process, and hydrologic modeling. This approach will be used in this study to assess future changes in hydrological extrems on the Hérault River catchment.

2.1.2 Climate change projections

Climate models represent in details physical atmospheric processes at the global scale (IPCC, 2013). Different types of climate models exist. In long term CC impact studies, the GCMs (General Circulation Models) are forced by greenhouse gas emission scenarios as inputs. To assess climatic projection quality and know if these projections are suitable for long term studies, climatic simulations are compared to observed data on a historical period. CMIP (Coupled Model Intercomparison Project) has developed a standardized and strong climate model protocol, to improve the availability and robustness of climate model outputs for scientists (https://www.wcrp-climate.org/). CMIP5 is the 4th phase of the project and is now the reference for impact studies, while CMIP3 is out-of-date. CMIP5 is based on RCP scenarios (Radiative Concentration Pathways) (see Moss et al., 2010). These scenarios were developed by first assessing levels of radiative forcing in the atmosphere at the end of the 21st century, and then associating the radiative trajectories with corresponding socioeconomic and gas emission scenarios. Terray and Boé (2013) present temperature and precipitation projections over France (Fig. 1), computed with GCM projections extracted from the CMIP5 database. A clear trend to an increase of up to 4.5°C at the end of the century is observed on temperature projections with RCP 8.5 (scenario without mitigation), whereas precipitations show no clear signal (Fig. 1). For RCP 4.5 (scenario with medium mitigation), the change in temperature reaches 2°C of warming

by the end of the 21st century. The lack of precision on rainfall projections comes from the GCM structure: while computation of temperatures is optimized, precipitation processes are not well reproduced by GCMs due to the complex physical, temporal, and spatial properties of these events (Kent et al., 2015). Regional Circulation Models (RCMs) provide CC projection at a higher spatial resolution on a specific region. However, the resolution is still too rough to well represent local meteorological events (Rauscher et al., 2010, see e.g.) for impact studies.

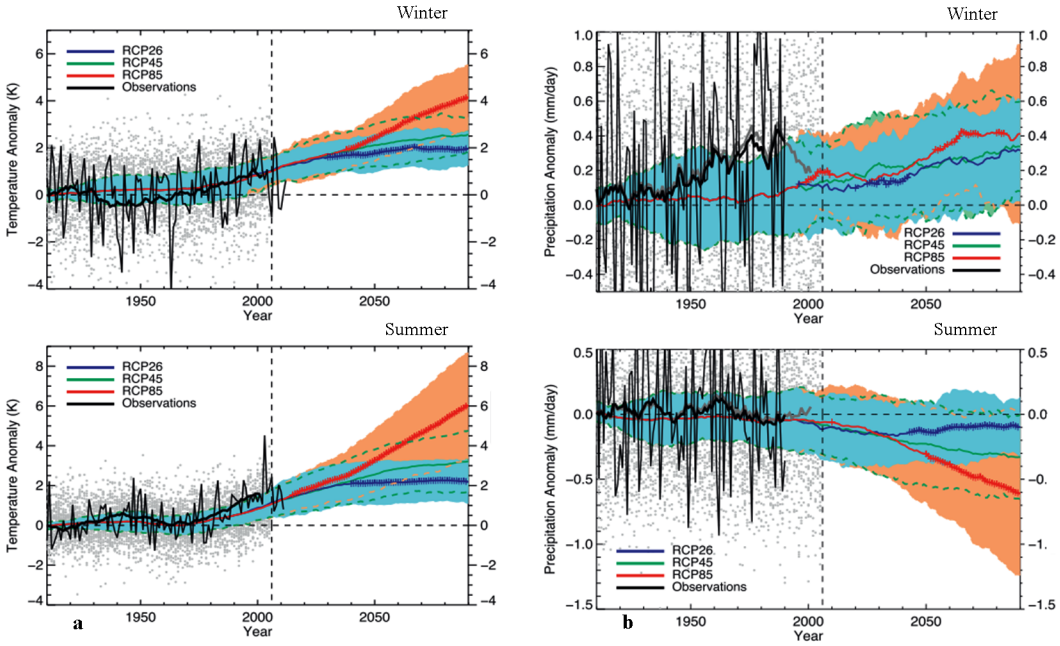

Figure 1: Time evolution of seasonal a) temperature and b) precipitation anomalies in France. Top in winter, bottom in summer.

Modified from Terray and Boé (2013)

2.1.3 Downscaling methods

The downscaling process is an important step since the spatial resolution of GCM cells is too coarse to take into account local meteorological processes (see e.g. Rauscher et al., 2010). GCMs have approximatively a 100km resolution, whereas RCMs (Regional Circulation Models) have a typical resolution of about 50km for the largest ones (see e.g. the regional climate model for the European region EUR-44) to 12,5km for the finest ones (see e.g. EUR-11). All EURO-CORDEX information is available on the website: https://euro-cordex.net. Some meteorological events are not well represented at coarse resolution, especially precipitations during storm events and snow precipitation on mountains. A finer spatial resolution describes better the topography, which can control local meteorological events (Montesarchio et al., 2014). Downscaling method draw a new grid at an higher spatial resolution. For example, in our case study, we will use the ADAMONT method (Verfaillie et al., 2017) based on the SAFRAN reanalysis data on an 8km grid resolution (Vidal et al., 2010). ADAMONT uses outputs from RCMs, and includes a statistical bias correction method.

There are two main categories of downscaling methods (see e.g. Duran, 2012). Dynamic downscaling uses climate model outputs as border conditions to create projections on a new high-resolution grid.

However, it requires a long computing time, and users need to know the physical parameters of local meteorological processes. Statistical methods are easier and faster than dynamic methods. They are based on a statistical relationship between climatic records at high and low-resolution. There is a large range of statistical methods: linear scaling, advanced delta change, or quantile mapping. Seguí et al. (2010) show that all those methods have different limits because they are based on different hypotheses. The common hypothesis is the stationary state: the correction function is constant over time, but in the CC context this assumption becomes irrelevant. It shows that the downscaled precipitation spatial patterns differ depending on the chosen method, and seasonal temperatures can differ as well with the method. It can be a significant source of uncertainty. The computed runoff series diverge with the methods and seasons in terms of anomaly: methods are disagreeing on the sign of runoff anomaly. Finally Rauscher et al. (2010) show that the amount of simulated precipitation is often overestimated with statistical downscalling.

Various approaches have been developed to adjust RCM outputs to observations (analog method, CDFt, quantile mapping...). Quantile mapping is widely used for bias correction since it is statistically efficient to adjust precipitation distribution. Hence, adjustment quality depends on data quality (Gudmundsson et al., 2012). In our case, for a partially mountainous catchment, the downscaling process is challenging due to strong and localized convective meteorological events (see e.g. Rauscher et al., 2010). In our study, we used ADAMONT (Verfaillie et al., 2017) outputs, drived from an innovating statistical method for the downscaling process. ADAMONT is built on RCM outputs and uses SAFRAN reanalysis data as model inputs (Verfaillie et al., 2017). SAFRAN is used to validate climate model outputs on a reference period and provides a reference for CC assessment due to their good quality and robustness (Vidal et al., 2010). SAFRAN reanalysis provides diverse climatic variables: rainfall, snowfall, solar radiation, humidity, and wind speed, temperature. The ADAMONT method initially developed by MétéoFrance is based on quantile mapping method, applied on the climatic variables provided by SAFRAN, and goes beyond the current limit of the stationary problem (Verfaillie et al., 2017). Quantile mapping is based on the statistical distributions of observations and simulations. Data simulation quantiles are adjusted with a transfer function, based on the quantiles of observation values corresponding to the same probability (Maraun, 2016). To overpass the stationary problem and improve the spatial-temporal consistency, this protocol was developped in nine steps (see Verfaillie et al., 2017).

2.2 Uncertainties in climate change impact study

2.2.1 Cascade of uncertainties

Generally, all modeling outputs include a part of uncertainty. There are three primary sources of uncertainty in a model which result in uncertainties on the outputs: 1) the model inputs; 2) the model structure, i.e. the equations; 3) the chosen parameter set during calibration. Moreover, in impact studies various models are used in a modeling chain, and each step generates uncertainties as shown on Fig. 2. According to Mitchell and Hulme (1999), "The unpredictability of the climatic and global systems introduces a cascade of uncertainty to regional climate prediction that cannot be squeezed to the single point of the 'single result' approach to prediction." This concept is a reference for CC impact studies. All the impact modeling chains include significant uncertainties that are cas-

caded from the first to the last stage. An evaluation of confidence intervals of CC impact outputs is necessary and is generally performed with an uncertainty analysis (UA). To evaluate uncertainties a multi-model approach is the norm (Teutschbein and Seibert, 2010): multi-model approach allows us to take into account the uncertainty due to representation of climate processes. The use of different hydrological models, with different spatial resolutions and structures, different calibration procedures, and various couples of climatic scenarios and models is required.

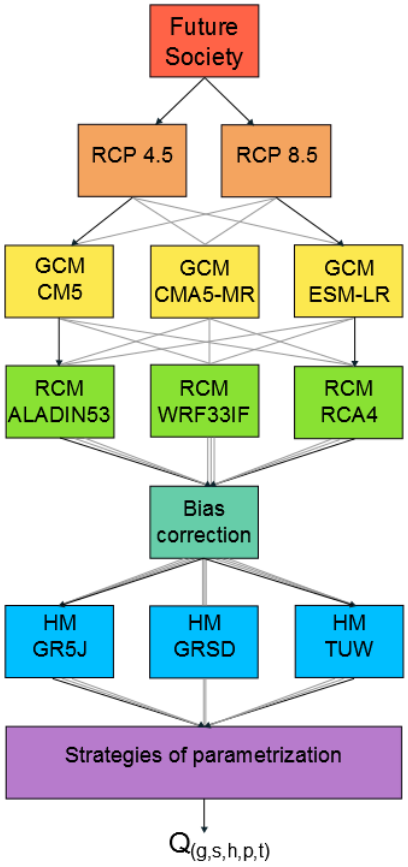

Figure 2: Schematic representation of the cascade of uncertainties, based on the method use in this study. Two RCPs used separately, three GCMs forced by RCPs, each GCM feed each RCM. Three RCMs used, but only one bias correction method used. After three HMs feed by climatic data to simulate streamflows. For each HM twenty-nine calibration strategies were used. RCP: Relative Concentration Pathway; GCM: Global Climate Model; RCM: Regional Climate Model; HM: Hydrological Model.

2.2.2 Probabilistic approach

To quantify the uncertainties and evaluate the rank of the contribution of each modeling step, two main approaches are generally used: historically, deterministic approaches have been widely used (Davies et al., 2009); (Dobler et al., 2012). This method is a simple screening method to explore sources of uncertainty one by one, and then rank the different uncertainty sources. Disadvantages of this method are various: interactions between parameters are not taken into account, and the ranges are not normalized. A better alternative is the use of probabilistic approaches, such as the one used by Vidal et al. (2016). The authors considered several possible scenarios and hydrological models (HMs), to generate with a stochastic approach a variable set for each combination (4 GCMs

and 3 downscaling methods). That was made possible by the large amount and sources of available data. After a re-sampling, they calculated hundreds of time-series projections for six different hydrological models. A specific index was calculated for low-flows and model uncertainties components were estimated with an ANOVA. This study improved the comprehension of uncertainties, as they found predominant uncertainty sources in internal variability at large and small scales for low-flow projections. Similarly, Parajka et al. (2016) studied hydrological models (HMs) and climate scenarios uncertainties in low-flow projections in Austria. They adopted a probabilistic approach coupled with an ANOVA. Different climatic scenarios, calibration procedures, and hundreds of catchments across Austria were used to compute a low-flow index. They concluded on different uncertainty sources contribution to low-flow projections according to the seasons. In summer, uncertainty is largely dominated by climate scenario gaz emission scenario (GES), whereas in winter contribution of HMs is of the same order of magnitude. Not only low-flow projections are studied in CC context but high-flows are studied too. Collet et al. (2017) assessed uncertainties on extreme flows in CC context with a probabilistic approach. To investigate events with a high return period, they used the extreme value theory and return period analysis, and quantified uncertainties related to the extreme value models and the climate model parameters. They concluded that uncertainty related to climate model and extreme value model are of the same order of magnitude, and that these sources of uncertainty need to be accounted for in impact studies.

2.2.3 The QE-ANOVA analysis

The quantification of different uncertainty sources are investigated with a multi-model approach ensemble of simulations resulting from a multi-scenario multi-model chain. In this study for a given GCM/RCM couple, an ensemble of HM projections is used to analyze future changes in hydrological response.

Firstly, time series of the variables of interest need to be provided by all the different GCM/RCM couples used. However, climatic projections can be missing for some GCM/RCM couples. In this case, the incomplete matrix of GCM/RCM projections used is challenging, and the quantification of uncertainties based on a parametric method like ANOVA can be biased, because some climatic models are more represented than others. To tackle this issue, Evin et al. (2019) developed the QUALYPSO method that deals with an incomplete matrix of climate model outputs. The approach is based on a data augmentation processe and it is adapted to hydrological projections.

The second challenging aspect of this procedure is how an ANAOVA analysis on uncertainties is conducted. A climatic projection can be considered as the sum of the climate response of a model at time t, and the deviation from the climate response obtained with a member of the modeling chain (Fig. 3). This highlights that the total uncertainty for an ensemble of projections is the combination of the uncertainties from the climate model response and the noise due to the climate natural variability (internal variability) (Eq. 1).

$$Y(g,s,t) = y(g,s,t) + \nu(g,s,t) \tag{1}$$

$$x(g,s,t) = y(g,s,t) - y(g,s,t_C) \tag{2}$$

With Y the climatic model output, y the climatic trend, and ν the residue of the fit of the climatic trend (deviation from the climatic response), g: GCM used, s: RCM used, h: HM used. The difference of climatic variable trend between the historical and the future period. This anomaly x is

used as the variable of interest for the uncertainty analysis. The quasi-ergonic ANOVA (QE-ANOVA) developed by Hingray et al. (2019); Evin et al. (2019) is based on this concept of climate response over time. QE-ANOVA improve the precision of estimations compared to previous ANOVA methods (e.g single time ANOVA), used to evaluate uncertainties in climate impact studies. However, some issues resulted from these approaches, especially the lack of temporal coherency.

The quasi-ergonic assumption establishes a time average along each trajectory that is described by a linear function; in the QE-ANOVA case, the trend model estimates the climatic response of the chain. According to Hingray et al. (2019) the general principles of QE-ANOVA are: first estimating a trend model over time, second determining the climate response, and finally, estimating the climate model internal variability. The climate response is defined as the trend model at the year of interest, and the internal variability is the variance over the time of residuals. The QE-ANOVA approach is chosen to characterize model uncertainty variance and estimate the contributions of each modeling step. Samples of interest are defined in different groups, and one observation is made on each group combination. In this study multi-modeling chain steps are considered as groups. This statistical method can determine whether group means differ, and which one differs from the others. Hingray et al. (2019) used QE-ANOVA on climatic projections (e.g. temperatures and precipitations) to evaluate uncertainties, but as shown by Vidal et al. (2016), QE-ANOVA is also adapted to hydrological projections. Vidal et al. (2016) examined the effects of: GCMs, bias correction method, and hydrological models. The corresponding ANOVA model is defined by the following equation (Eq. 3):

$$x(g, s, h, t) = \mu + \alpha(g, t) + \beta(s, t) + \gamma(h, t) + \epsilon \tag{3}$$

where x is the variable of interest, μ is the overall mean, α, β, γ, are the main group effect, and ϵ is the residual, or "error" between individual observation and combined groups effects.

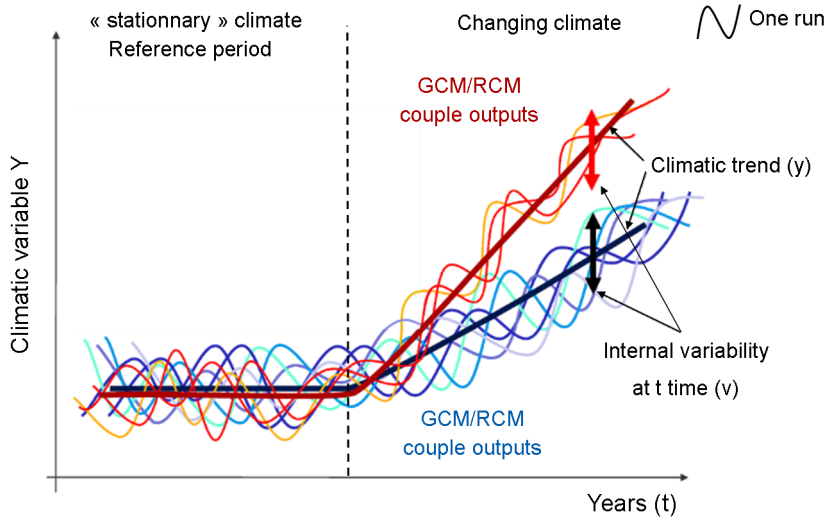

Figure 3: Schematic representation of the decomposition of the climatic signal with the QE-ANOVA method. Modified from Hingray framework.

3 Material and Methods

3.1 Study area : The Hérault River catchment

3.1.1 Geographical context

The Hérault River is located in the south of France (see Fig. 5). The outlet is located in Agde, in the Mediterranean Sea. The basin is delimited in the north by the Cévennes mountain range, Mont Aigoual (1 565m), which is the source of the Hérault River. The population living on the basin is around 170k inhabitants in 2012, on an area of about $2500\ \mathrm{km}^2$. On the upstream part, the basin is characterized by fractured bedrock. On the middle part, a karst system is well developed. On the downstream part, an alluvial system is dominant. Fig. 5c shows land use of the catchment: the downstream area is largely occupied by fruit and vineyard production, highly irrigated, while forest cover is dominant on the upstream part.

3.1.2 Hydrological and meteorological context

The hydrological dynamic of this catchment is typical of Mediterranean catchments (Fig. 4), with an influence from the Cévennes Mountains. We observe high precipitations in autumn and spring, where rainfall events can be intense due to the Cévennes mountains, and the spatial distribution of annual precipitations is widely contrasted from upstream to downstream, as shown in Fig. 5a (from above 1500mm/year in the upstream part, to reach less than 600mm/year in the downstream part). Precipitation on the Cévennes Mountains occurs during Mediterranean storms in autumn, and can cause impressive flash floods. In terms of temperatures, the regional mean is mild in winter (above 5°C) whereas summers are dry and hot (above 20°C). There is also a spatial pattern shown on Fig. 5c, with higher temperatures downstream and lower ones downstream. Hydrologic stations were chosen according to the hydrogeological context, the land cover, and the available time series. The downstream part of the catchment plays an essential role in water supply in the region Fig. 5b. Moreover for CC impact studies it is recommended to use 30-year records according to the World Meteorological Organization guidelines. For this CC impact study, four hydrological stations were chosen, each providing data on a 30 years period: The Arre River at Le Vigand, The Vis River at St-Laurent-le-Minier, The Hérault River at Laroque, and The Hérault River at Gignac see Fig. 5c. The baseline period is defined from 1990 to 2018.

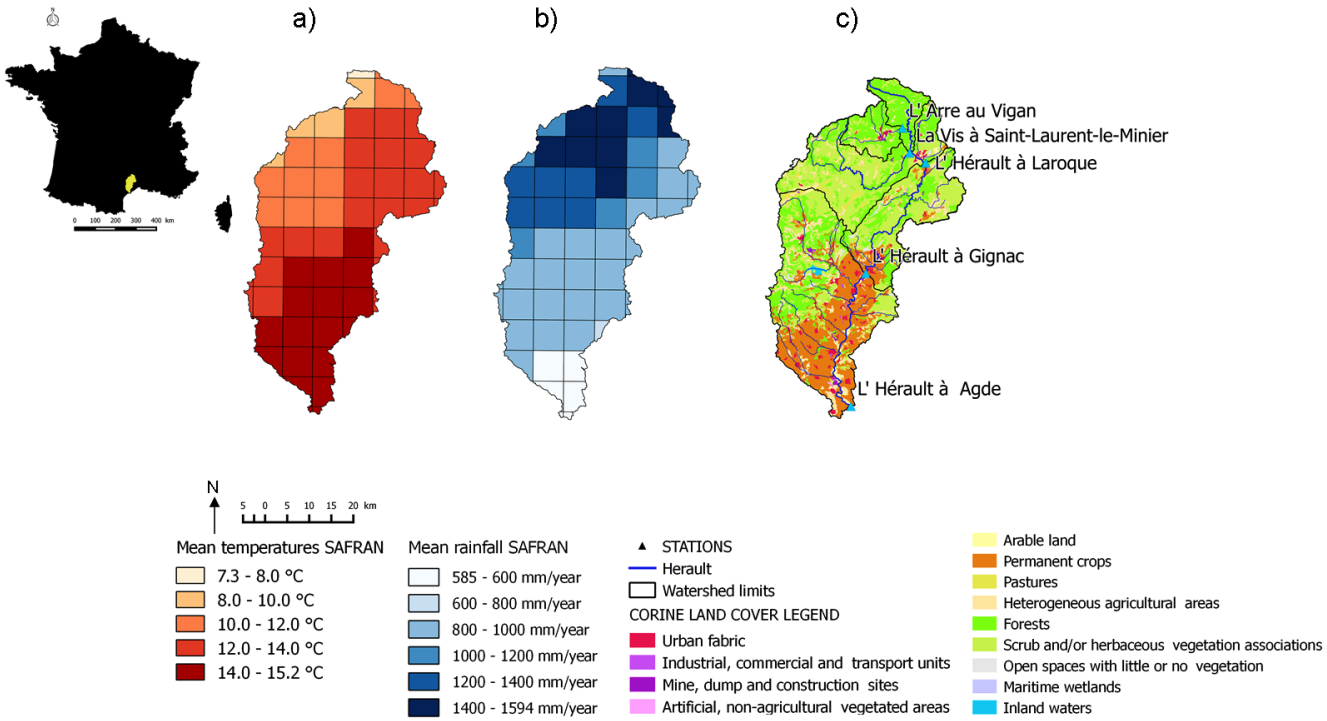

Figure 5: Maps of the Hérault River catchment: a) temperatures distribution, b) precipitation distribution, c) land use. Sources: SAFRAN, and Corine Land Cover 2018.

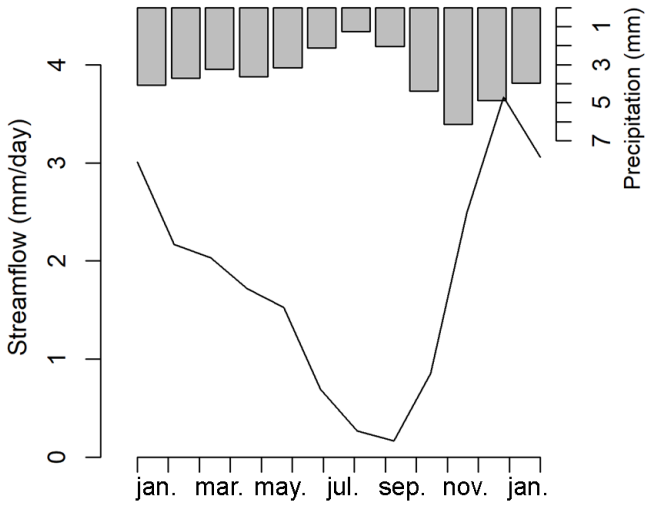

Figure 4: Annual hydrological dynamic of the Héraut River catchment

3.1.3 Data

The gauging stations and the time periods with available data are presented below in Table 1. We used the hydro-SAFRAN daily data set aggregated by IRSTEA, UR HYCAR (Delaigue et al., 2019). Météo-France provides climate data sets from 1958 to 2018 (SAFRAN meteorological reanalysis (Vidal et al., 2010)) and HYDRO DB provides streamflow records (Leleu et al., 2014). The climatic variables included: temperature, liquid and solid precipitations, and evapotranspiration. In this study the Penman-Monteith evapotranspiration was used. Hydrological data were available on four gaug-

ing stations, from 1986 or 1990 (see Tab. 1). Climatic projections are presented in Table 2, with the names of the different institutes, models, and scenarios. The spatial resolution of these projections is 0.11 degree (12.5km). Results were analyzed on a reference period (1976-2006) and future period (2006-2100), the Gignac station was used as the outlet of the catchment for the lumped HMs (GR5J, TUW), while the other stations were also used for the semi-distributed approach (GRSD).

Table 1: Available data for each gauging station.

Station name	Station code	Baseline period
The Arre River at Le Vigand	Y2015010	01/08/1986 - 31/07/2018
The Vis River at St-Laurent	Y2035010	01/08/1986 - 31/07/2018
The Hérault River at Laroque	Y2102010	01/08/1986 - 31/07/2018
The Hérault River at Gignac	Y2142010	01/08/1990 - 31/07/2018

Table 2: GCM-RCM couples used in this study. Source: https://www.hzg.de/ms/euro-cordex/

Institute name	RCM name	Driving GCM name	RCP scenarios
CNRM (France)	ALADIN53	CNRM-CM5	RCP 8.5 and 4.5
IPSL-INERIS (France)	WRF331F	IPSL-CM5A-MR	RCP 8.5 and 4.5
SMHI (Sweden)	RCA4	CNRM-CM5	RCP 8.5 and 4.5
SMHI (Sweden)	RCA4	IPSL-CM5A-MR	RCP 8.5 and 4.5
SMHI (Sweden)	RCA4	MPI-ESM-LR	RCP 8.5 and 4.5

3.2 Hydrological models

3.2.1 GR5J Cema Neige

GR5J (Le Moine, 2008) is a lumped conceptual rainfall-runoff model, with 5 parameters : the maximum capacity of production store (X1) in mm, the groundwater exchange coefficient (X2) in mm/d (X2 can be positive for a gain and negative for a loss of water), the capacity of routing store (X3) in mm, the unit hydrograph time constant (X4) in days, and another parameter to improve the representation of inter-catchment transfer with groundwater (X5), dimensionless (Fig. 6a). X1 is used to calculate the net precipitation input and the net evaporation output, then the water quantity in the production store is calculated with a balance equation. Next, the percolation is estimated with a classical streamflow equation, derived from the net precipitation and X1. The quantity of percolation is then split into two parts, and driven by two separate hydrographs: 90% of the flow are routed by the time hydrograph unit X4, and 10% are routed with a unit hydrograph. Streamflow is the sum of these two outputs. In order to represent streamflows seasonality due to snow process, GR5J was coupled with a snow routine, Cema Neige. The Cema Neige module has two parameters Ctg dimensionless and Kf (mm/°C), to represent snowmelt and snow accumulation.

3.2.2 GRSD

GRSD (Lobligeois et al., 2014) is a semi-distributed model based on GR5J (Fig. 6b). The main goal of a semi-distributed model is to take into account the spatial heterogeneity of the catchment, compared

to a lumped model. The studied catchment was divided into various sub-catchments, and each sub-catchment was fed with model inputs (meteorological data) and observed streamflow (De Lavenne et al., 2016, 2018). A lumped modeling process is applied on each sub-catchment or cell, to compute streamflow at the outlet of each cell and take into account the heterogeneity of the whole catchment (Fig. **??**). GRSD has seven parameters, five are the same as GR5J. Compared to GR5J, GRSD has two hydraulic additional parameters: C for celerity in m/s, and L for river length in m . The cells were created on each gauging station and used different parameter sets. According to De Lavenne et al. (2016) the performance of the is not necessarily better than the lumped model. Lobligeois et al. (2014) showed that GRSD semi-distributed model was more adapted for catchments with high rainfall spatial variability, in the case of high-flow studies, such as the Cévennes and the Mediterranean regions (substantial improvement was demonstrated for the Hérault River at Gignac).

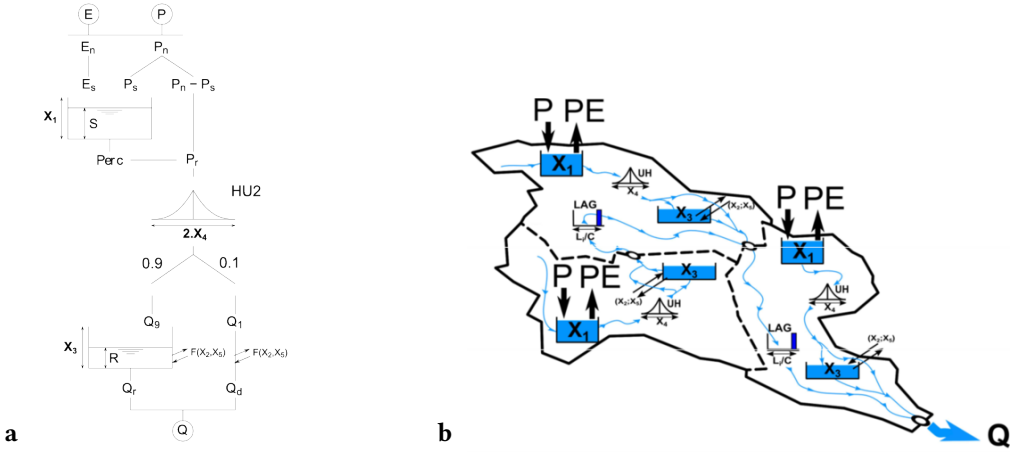

Figure 6: Presentation of a) GR5J and b) GRSD models (from Lobligeois et al., 2014)

3.2.3 TUW

TUW (Parajka et al., 2007) is a lumped conceptual rainfall-runoff model with 15 parameters (Fig. 7), and it is composed of three distinct modules:
- The snow routine has five parameters (SCF, DDF, Tr, Tm, and Ts), respectively a snow correction factor (demensionless), a degree-day factor (mm/°C/day), and three thresholds temperature (°C) to define liquid precipitation, solid precipitation, and snow melting. The snow routine computes the accumulation or the snow melt according to threshold temperatures. The precipitation and the snow melt (P_m) are routed to the soil moisture reservoir.

- The soil moisture routine has three parameters (LPrat, FC and Beta). The first one defines the limit of potential evapotranspiration (dimensionless); the second one is the soil moisture capacity called field capacity, and the third one is a runoff parameter. This routine computes the soil moisture with the amount of precipitation, meltwater, and evapotranspiration from the previous time step. The soil moisture routine control the actual evapotranspiration (E_A). E_A is calculated from the potential evapotranspiration and a linear function of the soil moisture. When the maximum FC (mm) is reached the routine generates runoff.

- The hydrological routine has seven parameters (k0, k1, k2, lsuz, cperc, bmax and cr free). k0, k1 , and k2 (mm) are storage coefficients, for the very fast, fast, and slow response respectively. lsuz (mm) is a threshold to start very fast runoff, cperc is the percolation coefficient (mm/day) , bmax (days) is the maximum base for low-flows and cr free a scalling parameter (days^2/mm). For more details and to have the description of the equations, see Parajka et al. (2007).

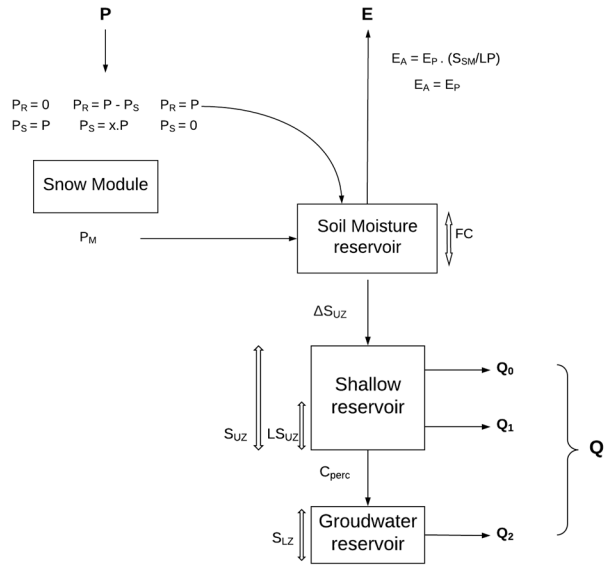

Figure 7: Presentation of the TUW model. P: Precipitations, PS: solid precipitations, P_M: water resulting from snow-melting, P_R: liquid precipitations, E: Evapotranspiration, E_P: Potential evaporation, E_A: Actual evaporation Q: Streamflow, FC: Field capacity

3.3 Modeling approach

3.3.1 Calibration-validation procedure

Different calibration procedures were used to generate multiple parameter sets in order to assess uncertainties due to model parametrisation:

- The split-sample test procedure was used. The input records and observed streamflow were divided into two periods of equal length, then the first one was used to calibrate and the second one to validate the model, and vice-versa. This procedure resulted in two parameters sets.
- The whole record was then used for one additional calibration and provided one parameter set.
- An alternative approach was used: the rolling calibration approach. For this procedure, the model was calibrated on a 10-year period, and the rest was used for validation, then the 10-year period was moved along 1 year, etc... It allows taking in account the variability due to temporal change, with different parameter sets (see e.g. De Lavenne et al., 2016). This procedure provided 19 parameter sets.

- The cross-validation procedure was used. We divided the records in n sub-periods, to calibrate on n-1 periods, and validate on the last one. This provide an estimation of the uncertainties in the estimation of parameters. This procedure provided 5 parameter stets.
- In order to evaluate uncertainties due to climate contrast between periods, two contrasted periods, the wettest and driest one, were defined. Then models were calibrated on each perio, resulting in two more parameter sets. According to Brigode et al. (2013) contrasted climatic periods have a huge influence on uncertainties for parameters transferring. Wet and dry periods were built based on the cumulative sum of monthly precipitation anomaly (Francois et al., 2018)(shown in appendix Fig. 24). Notice that the contrasted calibration periods are short.

In total this calibration protocol resulted in 29 different parameters sets, with different calibration-validation procedures to assess the model robustness. For each procedure a two-year warm-up period was used, to have a good initialization of the model internal variables.

We tested different streamflow transformations for the calibration/validation procedure (with Q the streamflow): Q, 1/Q, sqrt(Q) and a composite function (Q; 1/Q): Each of them has advantages: Q is more adapted for high-flows while 1/Q is more appropriate to low-flows. The objective function was chosen to be good enough for both low and high-flows, and the composite function (Q; 1/Q) seemed to be a good compromise.

In order to assess the quality of simulations, the Kling-Gupta Efficiency (KGE) (Gupta et al., 2009) was chosen (see Eq. 4), as a criteria for performance and robustness. This objective function was used for GR5J, GRSD, and TUW model for evaluation of parameters variability.

$$KGE = 1 - ED \tag{4}$$

$$ED = \sqrt{(r-1)^2(\alpha-1)^2(\beta-1)^2} \tag{5}$$

Where r is the coefficient of correlation, α is the ratio between the standard deviations of simulations and the standard deviation of observations, and β is the ratio between the mean of simulations and the mean of observations.

The composite function (C.F) can be written as follow:

$$C.F = \frac{KGE(Q) + KGE(1/Q)}{2} \tag{6}$$

3.3.2 Hydrological projections analysis

Hydrological projections are realised on the all period from 1992 to the horizon 2085. For the climatic projections the data observed are on the period 1992-2006, and compared to the future from 2006 to 2085. A rolling mean over 30 years was computed on these period to analyse the signal without the natural variability, indeed climate models are not suited to represent annual variability.

A yearly hydrological indicator was choosen for the QE-ANOVA on high and low-flows. For high-flows, the yearly threshold, defined with the upper 95th percentile (a streamflow value exceeded 5% of the time) was computed. For low-flows, the yearly Mean Annual 7-day Minimum flow (MAM7) was computed. The MAM7 is a yearly indicator used for low-flow analysis. The advantage of such indicator is that the mean of 7 days eliminates part of the daily variability.

3.3.3 Uncertainty analysis

The projected changes in streamflow were analyzed to compute the uncertainties on high and low-flows. A rolling average over 30 years was computed on the future horizon (2006-2100). This process was used to limit the inter-annual variability. The QUALYPSO method was used to fill the incomplete matrix of the different factors (GCMs, RCMs, HMs, Parameters) and to partition the total uncertainty. In the QE-ANOVA, the significance of each factor was tested, and four group effects were choose: GCMs, RCMs, HMs, and parameters. The factor levels of each group provided different outputs, and these responses were used to quantify sources of uncertainty and the relative importance of each factor over time. The residual variance, which is the part of the total variance that the ANOVA model can not explain, is included in the outputs. This residual variance is due to the model interactions.

The corresponding ANOVA model is defined on the following equation, the factor parameter set is now included in the QE-ANOVA :

$$x(g, s, h, p, t) = \mu + \alpha(g, t) + \beta(s, t) + \gamma(h, t) + \delta(p, t) + \epsilon \tag{7}$$

where x is the variable of interest, μ is the overall mean, α, β, γ, δ are the main group effect, and ϵ is the residual, or "error" between individual observation and combined groups effects.

4 Results

4.1 Calibration procedure

This section shows results of the calibration procedure for the three hydrological models over 1990-2018. The quantification and the assessment of the simulation quality is presented here, as well as the parameter sets resulting from the calibration procedure. Furthermore, the performance of the models and the obtained parameter sets are explored for different hydrological indicators, particularly for high and low-flows.

4.1.1 Annual streamflow

Simulations on different calibration-validation periods at the daily time step over 1990-2018 were compared to investigate the performance of the models and different calibration strategies. The comparison is based on C.F (Eq. 6) criterion with graphical representations of the rolling mean, shown on Fig. 8, Fig. 9, Fig. 10, for GR5J, GRSD, and TUW respectively. Simulations with GR5J and GRSD show a small envelope around the observations; and a good performance, with values between 0.5 and 0.9. It shows a good capacity of adaption to different calibration periods, in other words these models show a high performance. However for TUW model, simulations show lower criterion values. The graphic (Fig. 10) shows difficulties for the model to simulate flood peaks. The criterion has a large range of variation, from below 0.4 to 0.7. The TUW model calibrations present both unsatisfactory (0.4 < KGE < 0.6) and satisfactory simulations (0.65 < KGE < 0.75).

4.1.2 The parameter sets

Then we explored the parameters variability in accordance to the calibration-validation periods. The parameters were normalized with the upper and lower bounds, and shown on Fig. 8 for GR5J, Fig. 9 for GRSD, and Fig. 10 for TUW, to estimate the robustness of the calibration. The larger the variability of parameter sets over the calibration periods, the less they are capable of explaining the differences over the calibration periods. GR5J (Fig. 8b) shows for X3 a large variability, while X1 and X5 show a small variability, and X4 seems stable. X2 presents one extreme value, related to the parameter calibrated during the dry period. With GRSD (Fig. 9b) the distribution is different: X1, X2 and X3 have a greater variability compared to GR5J. The distributions of X4 and X5 are stable across the calibration procedures. The variability of parameters for TUW model is shown, but the parameters are different, so they are not comparable.

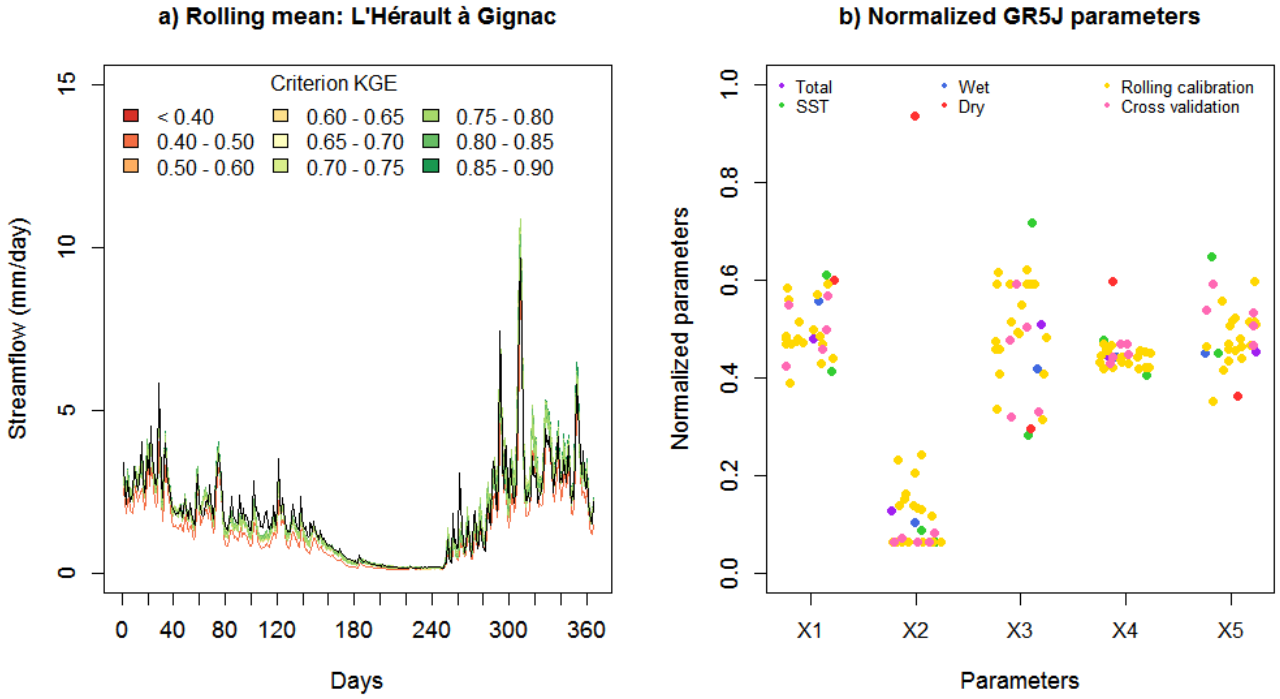

Figure 8: Calibration results for GR5J: The Hérault River at Gignac. a) Rolling mean values of streamflows over 1990-2018. Observations are in black and the colored curves represent distinct calibration-validation srategies. Colors indicate the goodness of criterion. b) Normalized parameters distribution. Color indicate the type of calibration procedure.

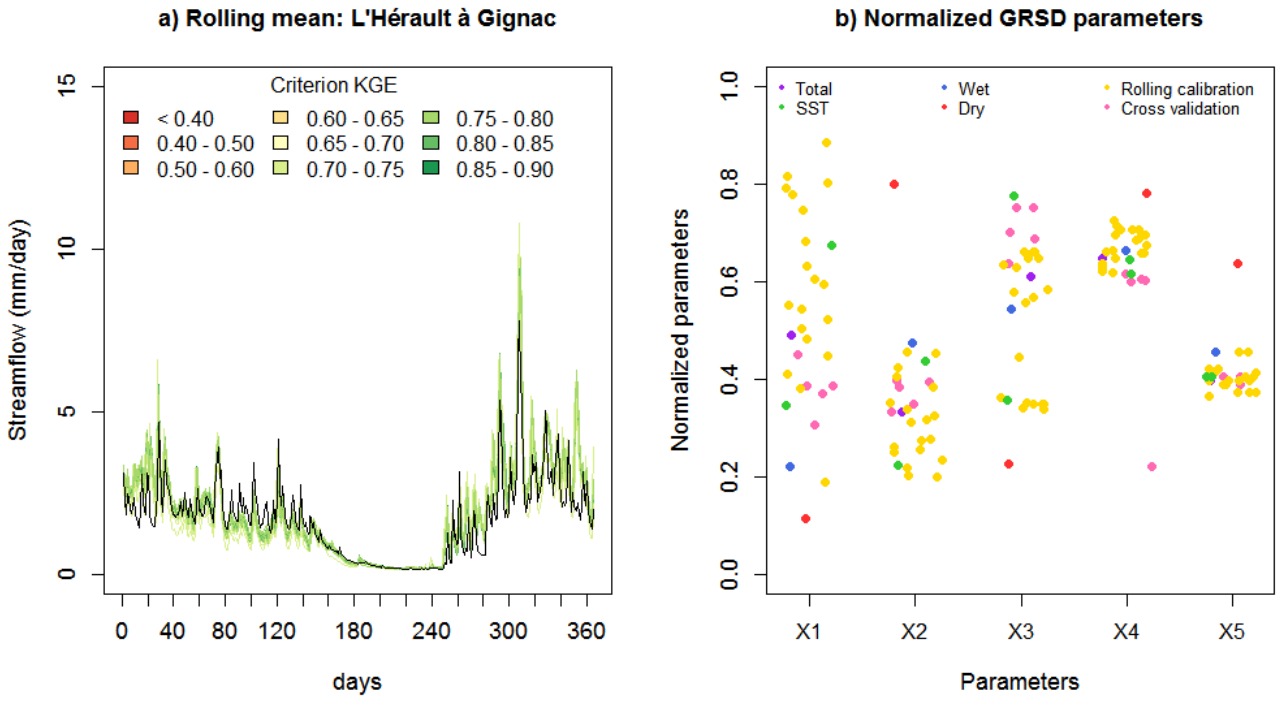

Figure 9: Results of the calibration procedure for GRSD: The Hérault River at Gignac. Same legend as the previous figure.

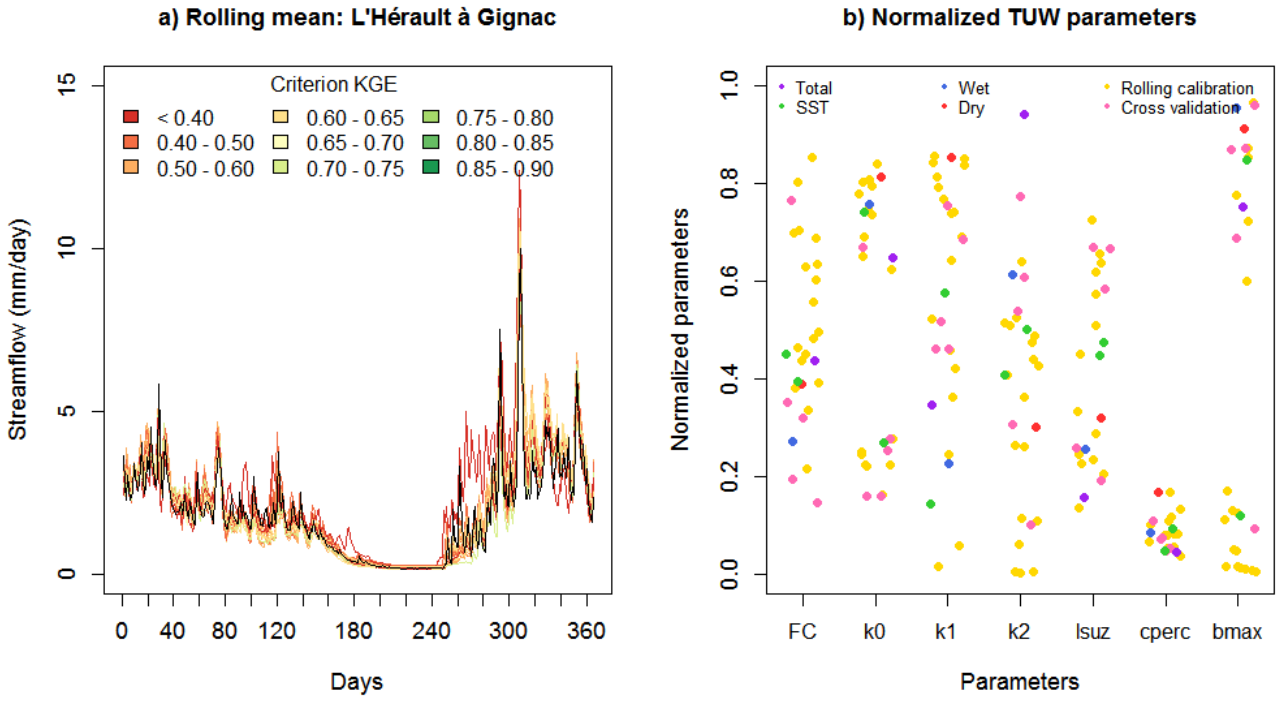

Figure 10: Results of the calibration procedure for TUW: The Hérault River at Gignac. Same legend as the previous figure. Notice that we plot only hydrological parameters except for cr free (the less sensitive one), and we added the soil moisture parameter.

4.1.3 High-flow and low-flow projections

This section compared simulated and observed streamflows over the reference period. It allows getting a better understanding of the bias generated by hydrological models and the choice of parameters. If GR5J and GRSD have shown excellent performances for their different parameters sets, it is not the case for all the parameter sets of TUW. However, for this study, the use of the three models is essential to analyze uncertainties related to hydrological models in a CC impact study. The hydrological model performance analysis is important to know which hydrological criterion is suitable and robust for assessing the evolution of discharges driven by climatic projections and make reasonable interpretations of results.

The hydrological models performance were explored in details for high and low-flows. We computed mean high-flow and low-flow indicators (i.e. Q95 and MAM7 respectively), for the different simulations resulting from different parameter sets and models. The flow duration curve (FDC) was computed for the models to show the quality of the representation of the extreme flows (Fig. 11). Moreover, time series of maximum and minimum simulated streamflows were built from the multiple simulations, to estimate the simulation range around the observed streamflow. The FDC of GR5J and GRSD present a small range between maximum and minimum values, whereas FDC of TUW shows a large range between both extrema. For GR5J and GRSD, high-flows are well simulated, while low-flows seem less well represented. For TUW, all the parameter sets can not represent the extreme flows.

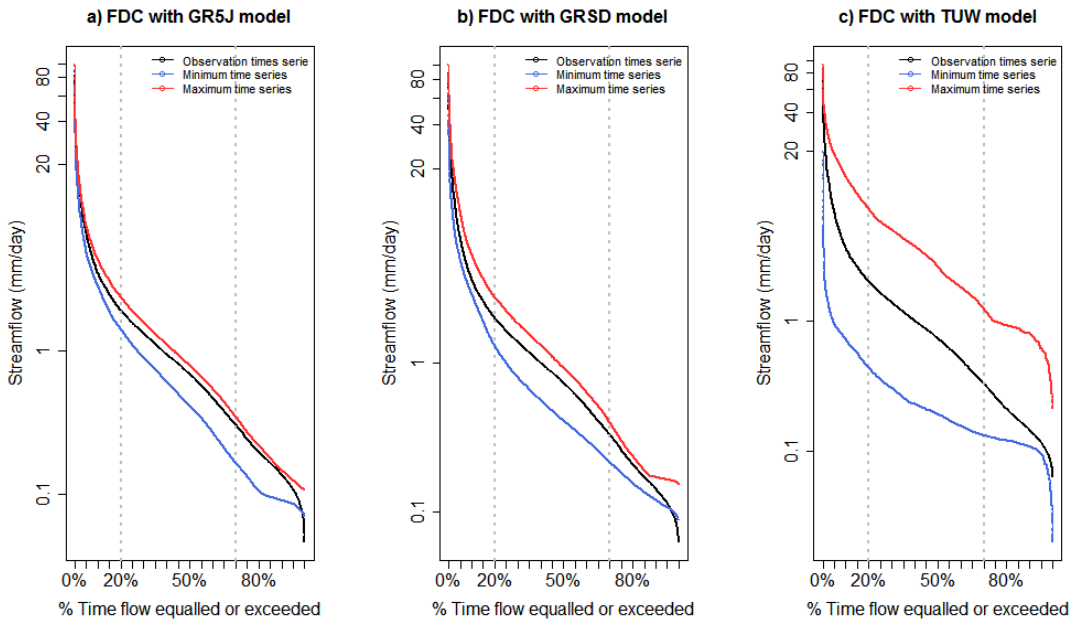

Figure 11: FDC for GR5J, GRSD, and TUW, for the Hérault River at Gignac. The maximum and minimum time series were built with the different simulations from all parameter sets.

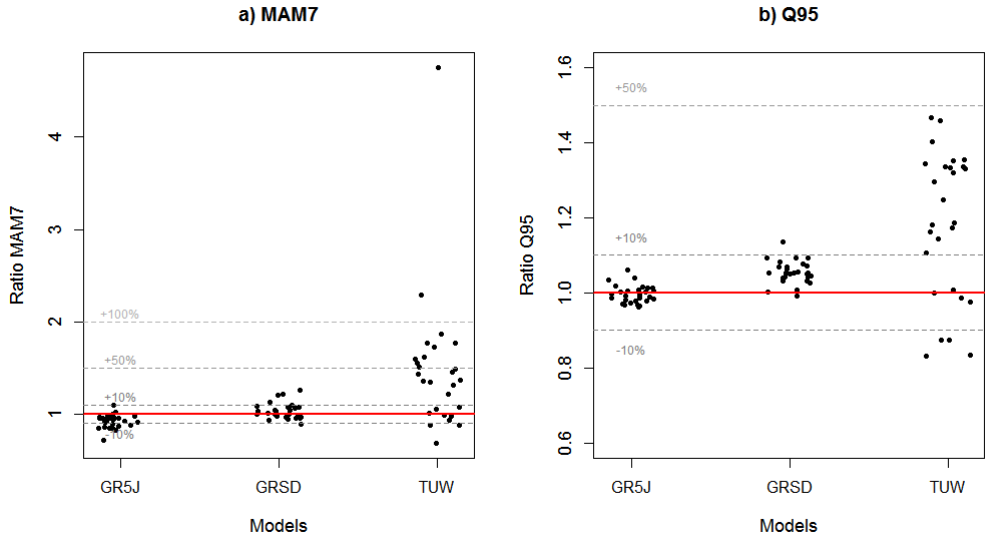

Figure 12: Comparison index, the ratio of means for high-flows and low-flows and the ratio of standard deviation for a) high-flows, and b) low-flows. Each dot represents one parameter set.

An index was calculated to estimate if the simulation is an underestimation or an overestimation. The index was the ratio of the simulated mean to the observed mean. Results are described in Fig. 12. If the index is below 1, simulations underestimate the streamflow and vice versa, if the index is above 1, simulations overestimate the streamflow. The most part of ratios computed with GR5J and GRSD outputs are included between -10% and, +10%. Low-flows computed with GR5J present a small underestimation, whereas high-flows computed with GRSD present a small overestimation. But the TUW model shows strong underestimations and overestimations for the different parameter sets. TUW model presents an overestimation of streamflows. For the low-flows 8 simulations are above 10%, 8 simulations are above 50%, and 2 simulations are above 100%. For the high-flows 20 simulations included between +10% and +50% for high-flows. The relative difference is more important for low-flows, but the absolute difference in volume is largely stronger for high-flows.

4.2 Hydro-climatic projections

4.2.1 Climatic projections

Mean temperature and mean precipitation projections on the Hérault River catchment are shown in Fig. 13, to assess the main future trend of these climatic variables. For RCP 4.5, the mean trend of temperature projections (Fig. 13a) is increasing over time, to reach a mean anomaly of +1.6°C by the end of the century (confidence bounds: +1.4°C to +1.8°C); and the mean trend of precipitation projections (Fig. 13c) shows a decrease over time to reach a daily mean anomaly of -0.25 mm/day by the end of the century. For scenario RCP 8.5, the mean trend of temperature (Fig. 13b) shows a higher increase of +3.5°C (confidence bounds: +2.8°C to +4.2°C). Regarding precipitation projections (Fig. 13d), the mean trend presents a decrease of -0.3mm/day by the end of the century. However, large uncertainties on precipitation projections make unclear the change in precipitations: the lower confidence bound shows no anomaly in precipitation, and the upper bound shows an important anomaly of -0.5 mm/day. The lack of significant changes in precipitation projections on the Hérault River catchment is an important conclusion for the interpretation of hydrological projections.

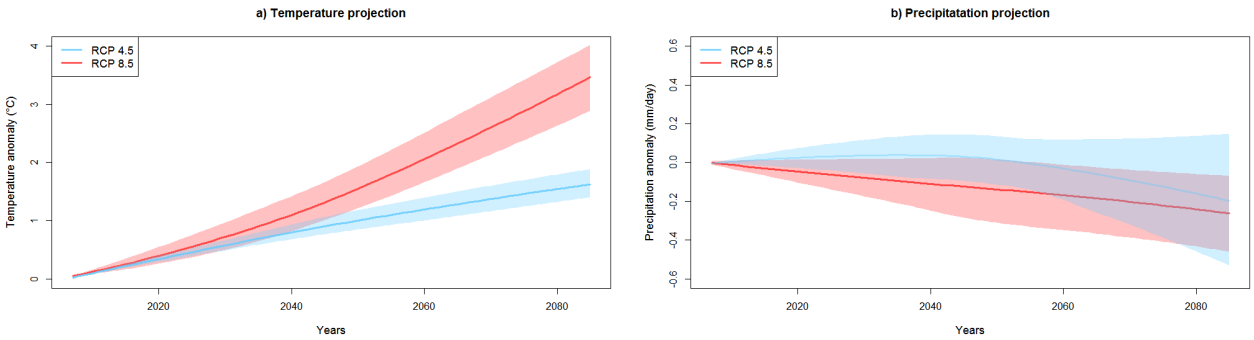

Figure 13: Mean trend over time of a) temperature projections, b) precipitation projections

4.2.2 Hydrological projections

Annual hydrological extreme projections are shown on Fig. 14. Looking at these two representations it don't allow us to note any specific trends or differences between RCPs used. Using these observations, the rolling mean over 30-years was computed, to have a mean trend and to conduct the uncertainty analysis with the QE-ANOVA method.

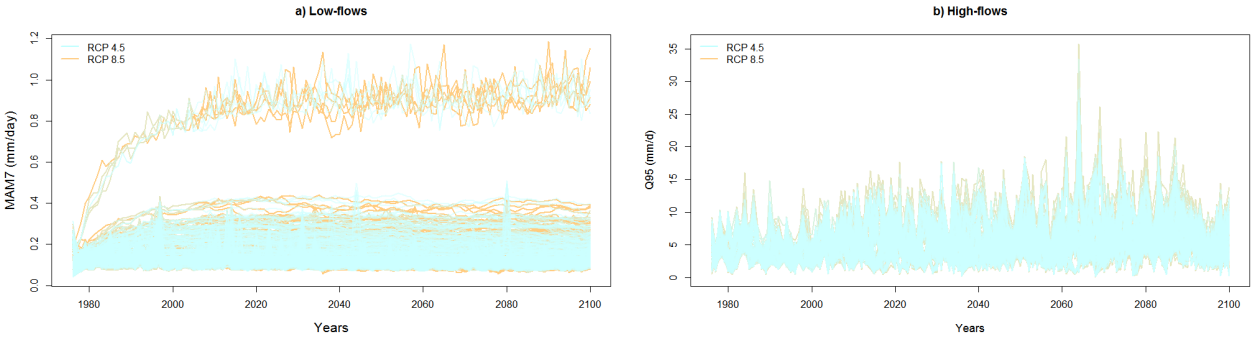

Figure 14: Annual hydrological projections a) for low-flows (MAM7), and b) for high-flows (Q95).

4.3 Uncertainty analysis

The total variance is decomposed following each source of uncertainty, and their relative contribution is represented in Fig.(15,and 16). The contribution of each source of uncertainty is changing over time. For RCP 4.5 Fig.(15) at the short lead time (before 2020), internal variability (in orange), HMs (in blue), and residual variance (in grey) are the main sources. The effect of GCMs (in yellow), RCMs (in green), and parameters (in purple) are minor. But at the end of century (2085), the residual variance becomes the main source of uncertainty. The contribution of HMs and Internal variability is decreasing over time, to becomes minor contribution. Unlike uncertainties related to GCMs, RCMs and parameters are increasing over time. However for RCP 8.5 (Fig. 16) the change in the contribution of each source of uncertainty is different. At the short lead time, RCMs, HMs, Internal variability and residual variance are the main contributors for uncertainties. This pattern is conserved over the time at the end of century HMs is the imprtant source of uncertainty followed by the residual variance and the RCMs. GCMs have only a small influence, and parameters too.

The Fig.(15; 16) shows the mean trend of the 30-year average changes in high-flows. For the RCP 4.5 Fig.(15), the trend is not representing any clear variation, the confidence bounds are covering

negative and positive anomaly, in the same proportion. So at the end of the century the anomaly on low-flow changes is not significant, no clear conclusion can be draw. The same observation can be made for low-flow projections with RCP 8.5, but the mean trend is negative, to reach -10% at the end of century, a small anomaly, not significant, due to the large confidence bounds.

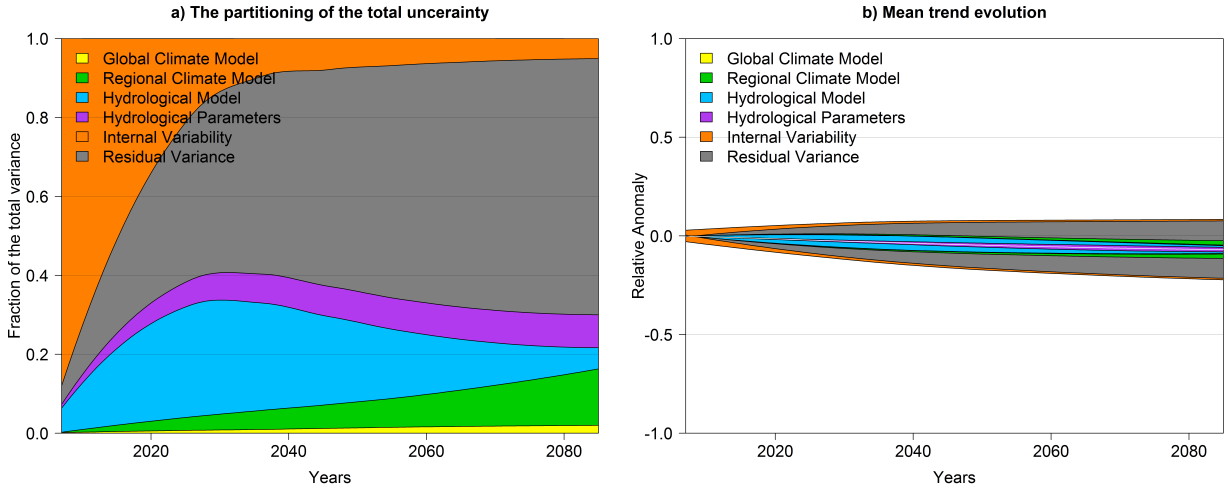

Figure 15: Uncertainty analysis on low flows RCP45.

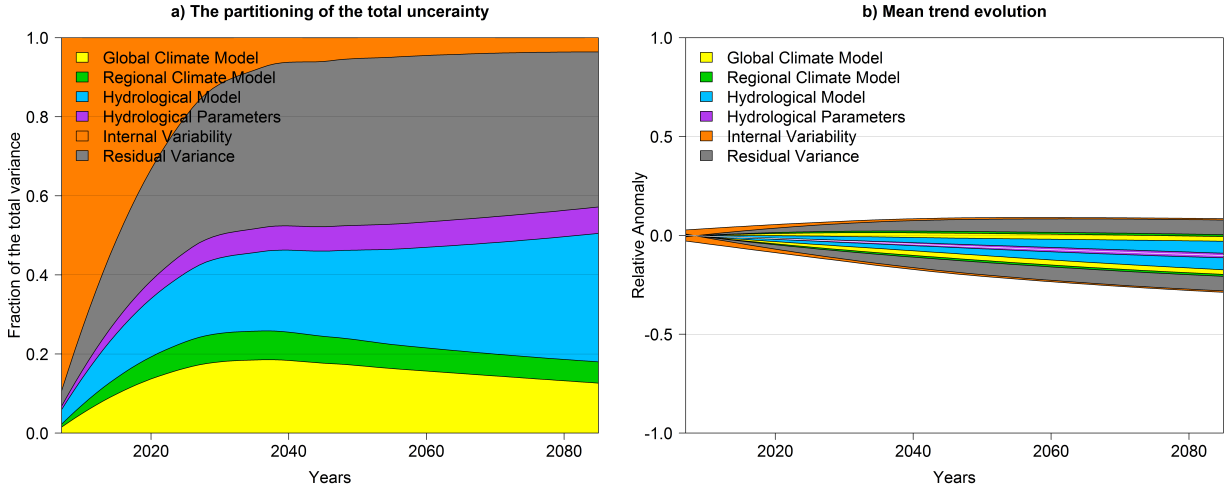

Figure 16: Uncertainty analysis on low flows RCP85.

The total uncertainties on high-flow projections until the end of the century compared to the historical periods, for two different RCPs. Fig. 17 shows the relative contribution of each source of uncertainty over time, for the rolling average over 30-years of high-flow changes with the RCP 4.5. The internal variability and the residual variance contribute for the most of the total uncertainty in the short lead time, they account respectively for less than 50% in 2020. Whereas at the end of the century the major source of uncertainty is the residual variance and HMs, they account respectively for 40% and 38%. The factor "Parameters" has a poor contribution to the total variance. GCMs and RCMs also have a small contribution. For RCP 8.5, results are shown on Fig. 18, at the short lead time the influence of GCMs/RCMs is larger than for RCP 4.5 (20% in 2020), whereas the part due to the residual variance is higher (30% in 2020), and the internal variability is the most important

(around 50% in 2020). For the end of century, GCMs/RCMs contribute for 15%, internal variability for 10% and residual variance for 50%, futhermore HMs and "parameter sets" contribute for 25% to the total uncertainty.

Fig. 17 for RCP 4.5, shows the mean trend of the 30-year average changes in high-flows. The figure shows an increase of high-flows over time, and the confidence bounds (90%) are increasing over time. At the end of the century, the anomaly computed is strictly positive and included between +5% to +70%. The simulated anomaly is strictly positive. Fig. 18 for RCP 8.5, shows the same trend, but not the same anomaly. The anomaly computed is included between an upper bound of +60% and a lower bound of -10%, but the mean trend is positive (+25%), the change in high-flow projections is not strictly positive.

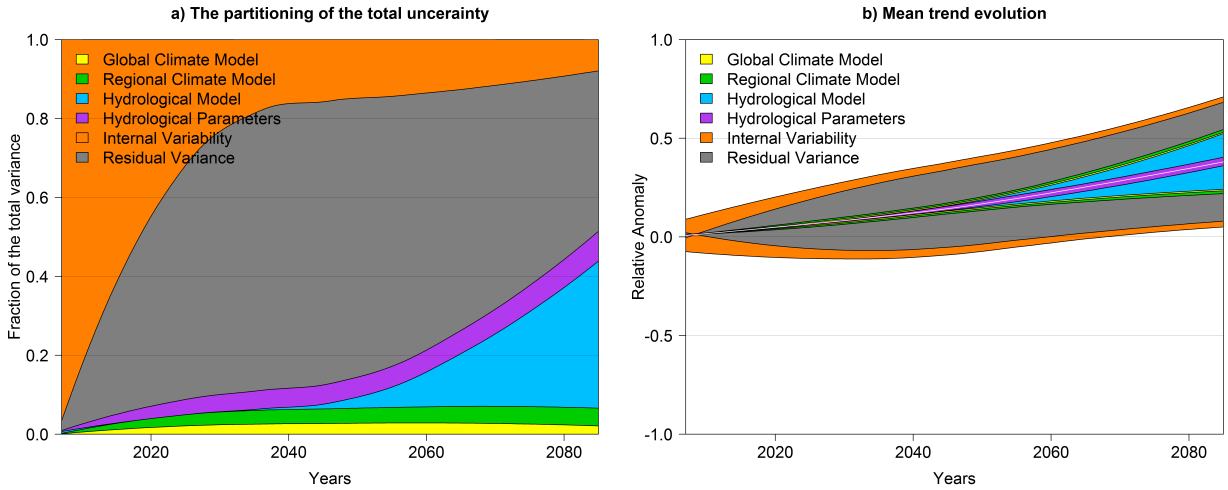

Figure 17: Uncertainty analysis on high flows RCP45.

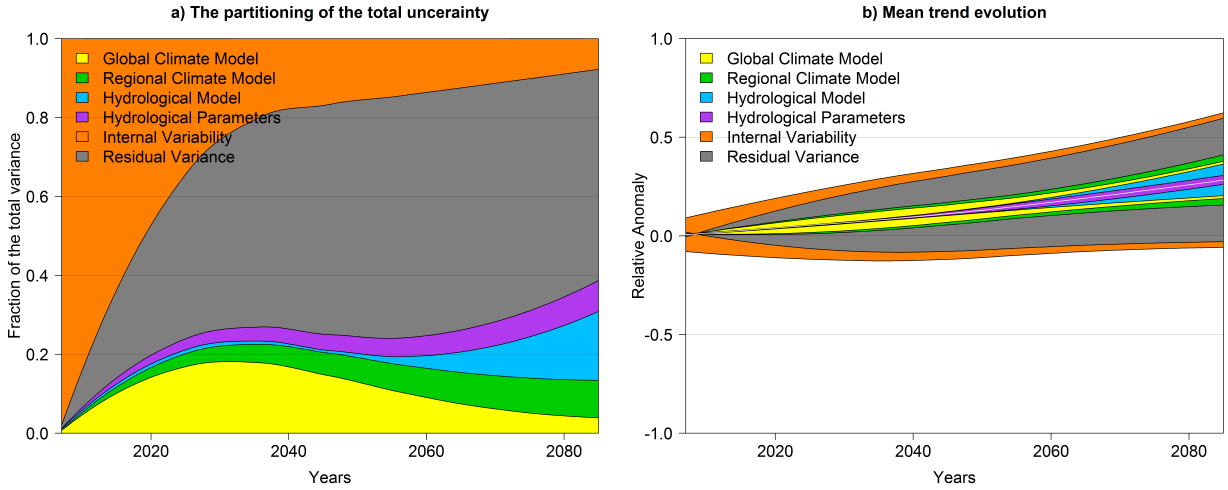

Figure 18: Uncertainty analysis on high flows RCP85.

5 Discussion

5.1 Sources of uncertainty analysis

To show how GCMs and RCMs can be a source of uncertainty it is interesting to look closer the relative difference in precipitation, and the difference in temperature between GCMs, and between RCMs, in the Héraut River basin. For the precipitations (Fig. 19) with the scenario RCP 4.5 MPI-ESM-LR is the driest model after 2060, but in the mid lead time, it is IPSL which is the driest one. The wettest GCM is CNRM-CM5. For RCP 8.5 (Fig. 20) the driest GCM is IPSL and the wettest is CNRM-CM5, they present an opposite behavior and an opposite relative difference. On (Fig. 20), the figures show an absolute difference of temperatures, for RCP 4.5 IPSL is the hottest GCM, and the other GCMs are very similar (Fig. 19). This trend is the same with the RCP 8.5. The data available were restricted to this three GCMs, but for future investigations, it is recommended to test more models in order to better quantify the part of uncertainties due to GCMs. The same analysis was done with the RCMS, note that for ALADIN53 and RCA4 are both wetter and hotter than WRF33IF, and are convergent.

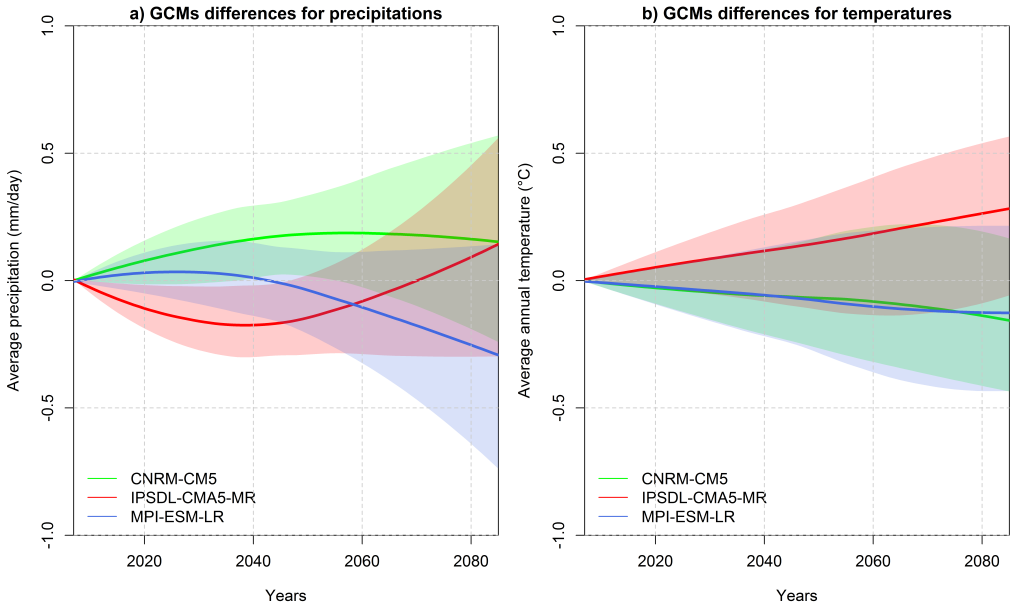

Figure 19: Relative differences between GCMs for RCP 4.5

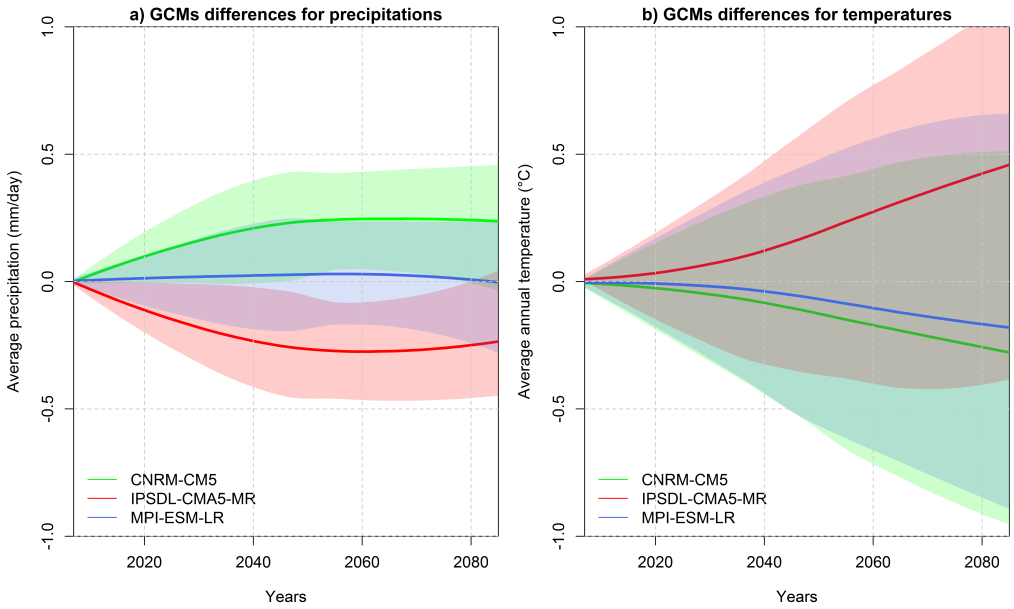

Figure 20: Relative differences between GCMs for RCP 8.5

5.2 Hydrological models performance and robustness

In order to better understand changes in the hydrological projections, low and high-flow indicators were compared for the three different hydrological models and their parameters (Fig. 21; Fig. 22). Four different periods are computed, the baseline, short lead time, mid lead time, and long lead time. As shown on the figure the evolution of the threshold (Q95), the indicator increase over the four periods and for the three hydrological models. For high-flow indicators the change is of same order of magnitude for the three hydrological models. However for low-flows, the change is not in the same magnitude for the three hydrological models, TUW model shows strong differences. For GR5J and GRSD the medians are decreasing according to the periods, and the medians are included between +15% and +10%, whereas for TUW the medians are closer to +20%, and the distribution of MAM7 are more extended to high values.

The lack of efficiency of TUW was shown in the results of calibration. With more investigation on this point, it appears that the objective function was not the optimal choice for this model. Indeed low-flow projections are better represented when the log transformation of streamflow with nash-sutcliffe is used as an objective function. Another point comes from the algorithm used for the optimization of the objective function (Ceola et al., 2015). It is a different algorithm compare to GR5J and GRSD. Finally, the TUW model structure is undoubtedly not very adapted to this Méditeranean catchment compare to GR models, but better adapted for mountainous catchment with a high contribution of snow-melt process, and not dry summer. The main difference between lumped model (GR5J) and semi-distributed model (GRSD) for hydrological projections is the simulation of more extreme values with GRSD compare to GR5J (Fig. 21; Fig. 22). Even if a model give more robust simulations, for a probabilistic approach it is necessary to consider different models, otherwise it will be a deterministic approach. Finally the contribution of parameters drove from different calibration strategies on the total uncertainties is never predominant (small for high-flow and non negligible for low-flow), previous studies awarded on the potential strong contribution of the parameters to the total uncertainty in climate change context, but this caution is correct for regions with a future decrease in among of precipitation around 20% (Dakhlaoui et al., 2017).

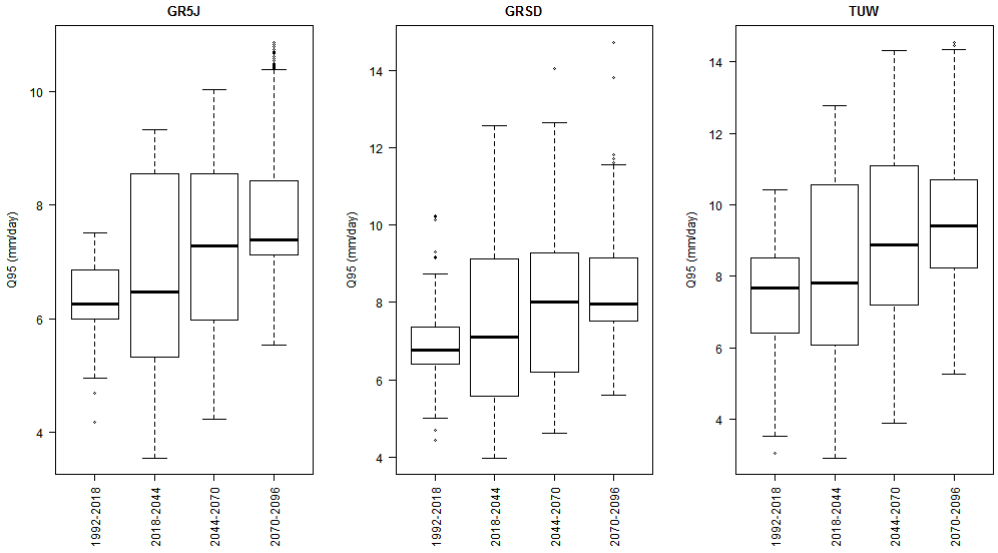

Figure 21: Hydrological models effect on threshold Q95 on different periods, with the different parameter sets

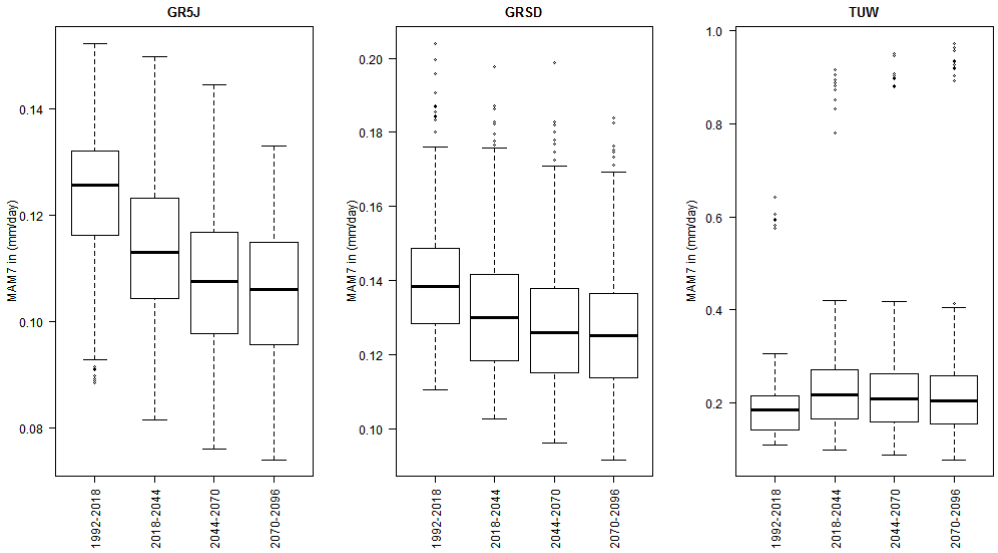

Figure 22: Hydrological models effect on MAM7 on different periods, with the different parameter sets

5.3 Significance of results: time of emergence

The QE-ANOVA is based on the normality assumption, but this statistical model is robust for large data sets. In order to check the validity of the assumptions, statistical tests were performed. The distributions of the residuals in all cases were analyzed, and large deviations from the normal distribution were found. The non-linearity of the hydrological models make sure of that, even if the rolling mean on precipitations show a normal distribution over time. Moreover, the statistical tests are sensible to the length of data, and can easily detect the variation. In order to conclude on the significance of results, the authors of the QE-ANOVA advise using another method called time of emergence.

Time of emergence, is a concept that was introduced by Hawkins and Sutton (2012), the ratio signal on noise is computed over time. The noise is defined as the root squared of the total variance and the signal as the mean trend over time. If the ratio is higher than one (or fewer than minus one), the signal is clear, and the results are robust. The ratio signal/noise was computed for the hydrological projections on high and low-flows (Fig. 23). Fig. 23a and Fig. 23b, show the ratio for high- flow projections, with the RCP 4.5 the ratio is increasing over time and becomes higher than one around 2050, so the projections are robust and significant after 2050. However, this is not the case for RCP 8.5, the ratio is increasing over time, but it still below to one. Finally for the low flow indicators (Fig. 23c, and Fig. 23d the ratio does not show any significant trend, but only a small decrease over time. Results are not significant for low-flows; it could be due to the sensibility of the catchment. Indeed the upstream the Gignac gauging station, the Hérault river catchment seems not to be sensitive to an increase in temperature, and low-flows are poorly affected by this change. These results are supported by the fact that the outlet of the study is located at Gignac (in the upstream part of the Hérault River catchment), because of on the downstream part of the basin is an alluvial plain, where the streamflows are affected by an increase of temperature. A large part of the upstream basin is coupled to a karstic system, wich could explain a low-flow replenishment during dry season.

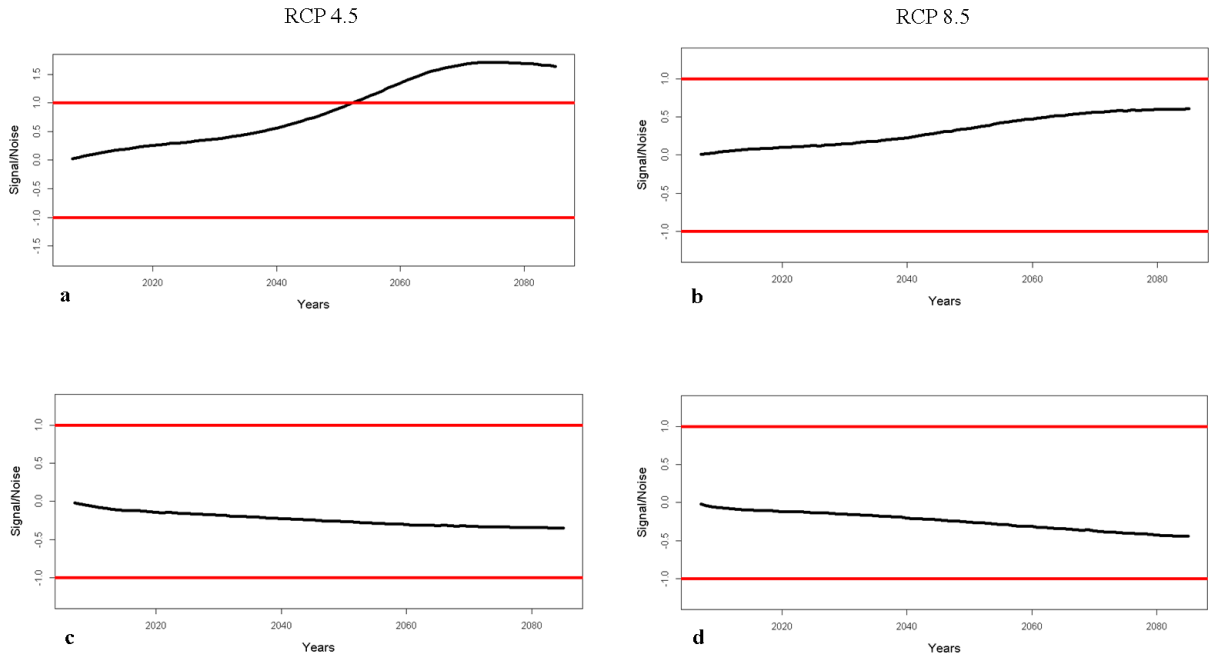

Figure 23: Ratio signal/noise for 30-years rolling averages of high-flow projections for a) RCP 4.5 and b) RCP 8.5. And of low-flows projections for c) RCP 4.5 and d) RCP 8.5.

5.4 Limits and contributions

In this study, the internal variability is assessed with only one run per GCM/RCM couple, so the estimation of the internal variability is biased. According to Hingray et al. (2019), it is preferable to use various run of the same climatic model to have a better estimation of the contribution of the internal variability to the total variance. For the next investigation, even if the QE-ANOVA can be carried out with only one run for each GCM/RCM couple, it is important to collect more members available for each GCM/RCM, in order to improve the assessment of the internal variability.

One step of the cascade of uncertainties that is not evaluated in this study is the downscaling method. All the climatic projections were downscaled with the same methods, ADAMONT. For future works, it is recommended to use multiple downscaling method to have different factor levels for the QE-ANOVA and assess the contribution of the downscaling step. However, users need to choose a downscaling method taking in account the characteristics of the catchment, and the stationary issues. For example, to represent local event (e.g Cevenol events) the downscalling method need to take in account the topography. For the future investigations it is recommended to use different downscaling method, to analyse all uncertainty sources. Another limit of this study is the hydrological indicator used to analyze the hydrological extremes. For future investigations, it is recommended to use a multi-factorial definition, and consider the frequency, the magnitude and the duration of the hydrological extremes (Collet et al., 2018).

The QE-ANOVA model used to quantify the contribution of each source of uncertainty has an important part of the total variance non-explained by the different factors, it is the residual variance. For the future investigations we have to test, the influence of the non-normality distribution of the hydrological indicators, and the number of factor levels used in the QE-ANOVA. The QE-ANOVA is driven with the rolling mean of hydrological indicators over 30-years to approach a normal distribution, but the normal distribution is not well reproduced, this implies to adapt the QE-ANOVA procedure to deal with non-normality. The levels of factors are very different: GCMs, RCMs, HMs have each 3 levels (3 models), but calibration strategies have 29 levels, this is a difference of one order of magnitude. This major difference can increase the interactions between factors and bias the statistical analysis.

The study has brought new results with the use of innovative methods. The previous projections on the Hérault River catchment, produced by Explore 2070 show different results: for high-flows (Q05), the relative change in the future (2046-2065), was estimated to decrease by 7% (min: -38% to max: +11%). In our study the trend is different, the new projections show an increase of the mean trend of high-flow indicators (based on the upper 95th percentile), the increase is around 20% in 2060 (min: 0% to max: 40%) for RCP 4.5 and, 10% in 2060 (min: -10% to max: 30%) for RCP 8.5. For low-flows projections our study shows no robust change, +10% to -15% in 2060 for RCP 4.5 and for RCP 8.5 +15% to -30%. Explore 2070 showed only -1% to -3%. The lower 10^{th} percentile was used in Explore 2070, whereas we chose the MMA7, which could explain part of the differences. But the main difference is the methodology: Explore 2070 did not use RCPs, rather SRES, the ADAMONT method used in our study was not available when Explore 2070 was conducted, and the hydrological model used for the Hérault River basin is a physical based model ISBA-MODCOU. Finally Explore 2070 did not use the QE-ANOVA. This comparison highlights the differences in the hydrological projections between Explore 2070 and our study, and these differences come from the methods and the tools used. The technical improvement of tools and models did not reduce the uncertainties on hydrological projections. However the use of the time of emergence, allowed us to compute significant impact on high-flow for decision makers whereas it highlights the difficulties to have clear conclusions for low-flows due to the sensibility of the catchment.

The previous study which used the same method is described by Vidal et al. (2016), the authors used the QE-ANOVA on the Durance River catchment, to study uncertainties on low-flows projections. They found a large contribution to the total uncertainties from the internal variability. But as explained above our estimation of the internal variability is biased due to the lack of available runs

for a given GCM. They didn't compute the part of uncertainties due to hydrological parameters, while our results show that parameter sets can have a non-negligible contribution. But our results are poorly significant on low-fow projections, as the change signal has he same magnitude than the noise. In the work of Vidal et al. (2016), they showed a decrease in yearly low-flows of about 20%, and their results are validated with the time of emergence analysis. The Héraut River catchment is less sensible than the Durance River catchment, to climate change impact on low-flows. An increase of temperature on the Méditeranean basin does not have the same consequence than for an Alpine water catchment. Our study highlights the differences in climate impact study due to the different hydrological processes in catchments.

6 Conclusion

This report described the methodology and the results of the new hydrological projections on the extremes, for the Héraut River catchment. The methodology used in the study was built to partition and to quantify the uncertainties on the projections, with the QE-ANOVA methodology.1) What is the impact of CC on hydrological extremes in the Hérault River catchment using recent climatic projections? The results show an increase in high-flow in the future, which could increase the flood risk. The relative increase of high-flow criterion is estimated to +5% to +70% at the end of the century with the RCP 4.5. For RCP 8.5 the anomaly is estimated to +60% to -10%. However for the low-flows and the related drought risk no clear trend is drawn, an anomaly of -10% for the mean trend with RCP 8.5, with large confidence intervals (+15% to -35%, relative anomaly). 2) What is the magnitude of uncertainties and where do they come from? High-flow projections with the RCP 4.5 are significant, but not robust with the RCP 8.5 as explained by the concept of time of emergence. The uncertainty sources weight are changing over time, over scenarios, and between high or low-flows. For high-flows evolution, HMs have a strong influence on the projections at the end on century, whereas internal variability and GCMs/RCMs have a higher influence at the short lead time. The contribution of uncertainty sources are different for low-flows, hydrological parameters seem to have a non-negligible influence, as well for HMs, and GCMs/RCMs. The internal variability presents poor contribution at the end of the century. 3) Can we draw conclusions for the decision makers? These results can be useful for the stakeholders to implement hydrological risk adaptation strategies, especially for high-flows, if they based their decision only on the previous studies they would not take into account the increase of high-flows with the climate change. In order to accelerate the adaptation to climate change, water managers need useful results, that include uncertainty, for their different managed basins.

References

Brigode, P., Oudin, L., and Perrin, C. (2013). Hydrological model parameter instability: A source of additional uncertainty in estimating the hydrological impacts of climate change? *Journal of Hydrology*, 476:410–425.

Ceola, S., Arheimer, B., Baratti, E., Blöschl, G., Capell, R., Castellarin, A., Freer, J., Han, D., Hrachowitz, M., Hundecha, Y., Hutton, C., Lindström, G., Montanari, A., Nijzink, R., Parajka, J., Toth, E., Viglione, A., and Wagener, T. (2015). Virtual laboratories: new opportunities for collaborative water science. *Hydrology and Earth System Sciences*, 19(4):2101–2117.

Chauveau, Chazot, Sébastien, Perrin, Charles, Bourgin, Pierre-Yves, Sauquet, Eric, Vidal, Jean-Philippe, Rouchy, Nathalie, Martin, Eric, David, Julian, Norotte, Thomas, Maugis, Pascal, and De Lacaze, Xavier (2013). Quels impacts des changements climatiques sur les eaux de surface en france à l´horizon 2070 ? *La Houille Blanche*, 4:5–15.

Collet, L., Beevers, L., and Prudhomme, C. (2017). Assessing the Impact of Climate Change and Extreme Value Uncertainty to Extreme Flows across Great Britain. *Water*, 9:1–16.

Collet, L., Harrigan, S., Prudhomme, C., Formetta, G., and Beevers, L. (2018). Future hot-spots for hydro-hazards in Great Britain: A probabilistic assessment. *Hydrology and Earth System Sciences*, 22(10):5387–5401.

Collet, L., Ruelland, D., Estupina, V. B., Dezetter, A., and Servat, E. (2015). Water supply sustainability and adaptation strategies under anthropogenic and climatic changes of a meso-scale Mediterranean catchment. *Science of the Total Environment*, 536:589–602.

Dakhlaoui, H., Ruelland, D., Tramblay, Y., and Bargaoui, Z. (2017). Evaluating the robustness of conceptual rainfall-runoff models under climate variability in northern Tunisia. *Journal of Hydrology*, 550:201–217.

Davies, H. N., Kay, A. L., Bell, V. A., and Jones, R. G. (2009). Comparison of uncertainty sources for climate change impacts : flood frequency in England. *Climatic Change*, 92(1):41–63.

De Lavenne, A., Lobligeois, F., and Collet, L. (2018). GUIDE D ' UTILISATION DE GRSD. Technical Report 2014, IRSTEA, UR HYCAR.

De Lavenne, A., Thirel, G., Andréassian, V., Perrin, C., and Ramos, M. H. R. (2016). Spatial variability of the parameters of a semi-distributed hydrological model To cite this version : HAL Id : hal-01342122 Spatial variability of the parameters of a semi-distributed hydrological model. *Proceedings of the International Association of Hydrological Sciences*, 373:87–94.

Delaigue, O., Génot, B., Lebecherel, L., Brigode, P., and Bourgin, P. (2019). Base de données hydroclimatiques observées à l'échelle de la france. *Comptes Rendus Geoscience*.

Diffenbaugh, N. S. and Giorgi, F. (2012). Climate change hotspots in the cmip5 global climate model ensemble. *Climatic Change*, 114(3):813–822.

Dobler, C., Hagemann, S., Wilby, R. L., and St, J. (2012). Quantifying different sources of uncertainty in hydrological projections in an Alpine watershed. *Hydrology and Earth System Sciences*, 16(11):4343–4360.

Duran, S. K. (2012). Capítulo 3 : Afrontando los retos. *GINDEV: Evaluación de la metodología Scrum en el desarrollo de videojuegos independientes*, 93(5):28–50.

Edenhofer, O., Pichs-Madruga, R., Sokona, Y., Seyboth, K., Kadner, S., Zwickel, T., Eickemeier, P., Hansen, G., Schlömer, S., and von Stechow, C. (2011). *Renewable energy sources and climate change mitigation: Special report of the intergovernmental panel on climate change*. Cambridge University Press.

Evin, G., Hingray, B., Blanchet, J., Eckert, N., Morin, S., and Verfaillie, D. (2019). Partitioning uncertainty components of an incomplete ensemble of climate projections using data augmentation. *Journal of Climate*, 32(8):2423–2440.

Francois, D., Drogue, G., and Delus, C. (2018). Projet CHIMERE21 : Calage de PRESAGES Calage unique.

Gudmundsson, L., Bremnes, J. B., Haugen, J. E., and Skaugen, T. E. (2012). Technical Note : Downscaling RCM precipitation to the station scale using quantile mapping – a comparison of methods. *Hydrology and Earth System Sciences*, 16(9):6185–6201.

Gupta, H. V., Kling, H., Yilmaz, K. K., and Martinez, G. F. (2009). Decomposition of the mean squared error and NSE performance criteria: Implications for improving hydrological modelling. *Journal of Hydrology*, 377(1-2):80–91.

Haddeland, I., Heinke, J., Biemans, H., Eisner, S., Flörke, M., Hanasaki, N., Konzmann, M., Ludwig, F., Masaki, Y., Schewe, J., Stacke, T., Tessler, Z. D., Wada, Y., and Wisser, D. (2014). Global water resources affected by human interventions and climate change. *Proceedings of the National Academy of Sciences*, 111(9):3251–3256.

Hattermann, F. F., Vetter, T., Breuer, L., Su, B., Daggupati, P., Donnelly, C., Fekete, B., Flörke, F., Gosling, S. N., Hoffmann, P., Liersch, S., Masaki, Y., Motovilov, Y., Müller, C., Samaniego, L., Stacke, T., Wada, Y., Yang, T., and Krysnaova, V. (2018). Sources of uncertainty in hydrological climate impact assessment: a cross-scale study. *Environmental Research Letters*, 13(1):015006.

Hawkins, E. and Sutton, R. (2012). Time of emergence of climate signals. *Geophysical Research Letters*, 39(1).

Hingray, B., Blanchet, J., Evin, G., and Vidal, J.-P. (2019). Uncertainty component estimates in transient climate projections. *Climate Dynamics*.

IPCC (2013). *Full Report*, page 1535 pp. Cambridge University Press, Cambridge, United Kingdom and New York, NY, USA.

IPCC (2014). *Summary for Policymakers*, book section SPM, pages pp. 1–32. Cambridge University Press, Cambridge, United Kingdom and New York, NY, USA.

Kent, C., Chadwick, R., and Rowell, D. P. (2015). Understanding uncertainties in future projections of seasonal tropical precipitation. *Journal of Climate*, 28(11):4390–4413.

Le Moine, N. (2008). *Le bassin versant de surface vu par le souterrain : une voie d'amélioration des performances et du réalisme des modèles pluie-débit?* PhD thesis. Thèse de doctorat dirigée par Andréassian, Vazken Hydrologie Paris 6 2008.

Leleu, I., Tonnelier, I., Puechberty, R., Gouin, P., Viquendi, I., Cobos, L., Foray, A., Baillon, M., and Ndima, P. O. (2014). La refonte du système d ' information national pour la gestion et la mise à disposition des données hydrométriques. *La Houille Blanche*, 1:25–32.

Lespinas, F., Ludwig, W., and Heussner, S. (2014). Hydrological and climatic uncertainties associated with modeling the impact of climate change on water resources of small Mediterranean coastal rivers. *Journal of Hydrology*, 511:403–422.

Lobligeois, F., Andréassian, V., Perrin, C., Tabary, P., and Loumagne, C. (2014). When does higher spatial resolution rainfall information improve streamflow simulation? An evaluation using 3620 flood events. *Hydrology and Earth System Sciences*, 18(2):575–594.

Maraun, D. (2016). Bias correcting climate change simulations - a critical review. *Current Climate Change Reports*, 2(4):211–220.

Milano, M., Ruelland, D., Fernandez, S., Dezetter, A., Fabre, J., and Servat, E. (2012). Facing climatic and anthropogenic changes in the Mediterranean basin: What will be the medium-term impact on water stress? *Comptes Rendus Geoscience*, 344(9):432–440.

Mitchell, T. D. and Hulme, M. (1999). Predicting regional climate change : living with uncertainty. *Progress in Physical Geography: Earth and Environment*, 23(1):57–78.

Montesarchio, M., Zollo, A. L., Bucchignani, E., Mercogliano, P., and Castellari, S. (2014). Performance evaluation of high-resolution regional climate simulations in the alpine space and analysis of extreme events. *Journal of Geophysical Research: Atmospheres*, 119(6):3222–3237.

Moss, R. H., Edmonds, J. A., Hibbard, K. A., Manning, M. R., Rose, S. K., Vuuren, D. P. V., Carter, T. R., Emori, S., Kainuma, M., Kram, T., Meehl, G. A., Mitchell, J. F. B., Nakicenovic, N., Riahi, K., Smith, S. J., Stouffer, R. J., Thomson, A. M., Weyant, J. P., and Wilbanks, T. J. (2010). change research and assessment. *Nature*, 463(7282):747–756.

Parajka, J., Blaschke, A. P., Blöschl, G., Haslinger, K., Hepp, G., Laaha, G., Schöner, W., Trautvetter, H., Viglione, A., and Zessner, M. (2016). Uncertainty contributions to low-flow projections in Austria. *Hydrology and Earth System Sciences*, 20(5):2085–2101.

Parajka, J., Merz, R., and Blöschl, G. (2007). Uncertainty and multiple objective calibration in regional water balance modelling: case study in 320 austrian catchments. *Hydrological Processes*, 21(4):435–446.

Piras, M., Mascaro, G., Deidda, R., and Vivoni, E. R. (2014). Quantification of hydrologic impacts of climate change in a Mediterranean basin in Sardinia, Italy, through high-resolution simulations. *Hydrology and Earth System Sciences*, 18(12):5201–5217.

Rauscher, S. A., Coppola, E., Piani, C., and Giorgi, F. (2010). Resolution effects on regional climate model simulations of seasonal precipitation over europe. *Climate Dynamics*, 35(4):685–711.

Sauquet, E. (2015). R^2D^2 2050 Risque, ressource en eau et gestion durable de la Durance en 2050. In *RéférenceS : Les connaissances scientifiques au service de la*, pages 47–55. Direction de la recherche et de l'innovation (DRI) du Commissariat.

Schewe, J., Heinke, J., Gerten, D., Haddeland, I., Arnell, N. W., Clark, D. B., Dankers, R., Eisner, S., Fekete, B. M., Colón-González, F. J., Gosling, S. N., Kim, H., Liu, X., Masaki, Y., Portmann, F. T., Satoh, Y., Stacke, T., Tang, Q., Wada, Y., Wisser, D., Albrecht, T., Frieler, K., Piontek, F., Warszawski, L., and Kabat, P. (2014). Multimodel assessment of water scarcity under climate change. *Proceedings of the National Academy of Sciences*, 111(9):3245–3250.

Scoccimarro, E., Gualdi, S., Bellucci, A., Zampieri, M., and Navarra, A. (2016). Heavy precipitation events over the Euro-Mediterranean region in a warmer climate: results from CMIP5 models. *Regional Environmental Change*, 16(3):595–602.

Seguí, P. Q., Ribes, A., Martin, E., Habets, F., and Boé, J. (2010). Comparison of three downscaling methods in simulating the impact of climate change on the hydrology of Mediterranean basins. *Journal of Hydrology*, 383(1-2):111–124.

Sellami, H., Benabdallah, S., La Jeunesse, I., and Vanclooster, M. (2016). Quantifying hydrological responses of small Mediterranean catchments under climate change projections. *Science of The Total Environment*, 543:924–936.

Terray, L. and Boé, J. (2013). Quantifying 21st-century france climate change and related uncertainties. *Comptes Rendus Geoscience*, 345(3):136 – 149.

Teutschbein, C. and Seibert, J. (2010). Regional climate models for hydrological impact studies at the catchment scale: A review of recent modeling strategies. *Geography Compass*, 4(7):834–860.

Verfaillie, D., Déqué, M., Morin, S., and Lafaysse, M. (2017). The method ADAMONT v1.0 for statistical adjustment of climate projections applicable to energy balance land surface models. *Geoscientific Model Development*, 10(11):4257–4283.

Vidal, J. P., Hingray, B., Magand, C., Sauquet, E., and Ducharne, A. (2016). Hierarchy of climate and hydrological uncertainties in transient low-flow projections. *Hydrology and Earth System Sciences*, 20(9):3651–3672.

Vidal, J.-P., Martin, E., Franchistéguy, L., Baillon, M., and Soubeyroux, J.-M. (2010). A 50-year high-resolution atmospheric reanalysis over France with the Safran system. *International Journal of Climatology*, 30(11):P. 1627–1644. DOI: 10.1002/joc.2003.

www.eaurmc.fr (2014). *les plans de bassins d'adaptation au changement climatique dans le domaine de l'eau. BASSIN RHÔNE-MÉDITÉRRANÉE*. DREAL délégation du bassin Rhône-Méditerranée, l'Agence de l'eau Rhône Méditerranée Corse, les DREAL des régions Bourgogne, Languedoc-Roussillon, Franche-Comté, Rhône-Alpes, Provence-Alpes-Côte d'Azur, l'Agence Régionale de Santé Rhône-Alpes, la DRAAF Rhône-Alpes, et l'Onema-DAST.

7 Appendix: additional figures

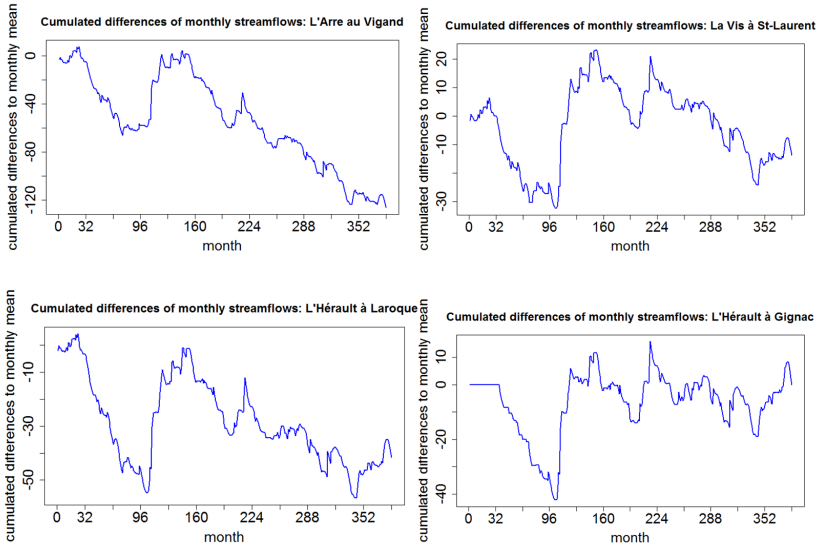

Figure 24: Cumulative sum of daily anomaly in streamflow compare to the monthly mean